New Zealand Acoustics

Volume 25, 2012 / #4

Neural Correlates of Noise Annoyance and Sensitivity

Sound Field of a Directional Source in a Reverberant Room

Improving Acoustic Insulation

Using Vibration-Damping Infills in Floors

ISSN 0113-8359

SignalCalc ACE

QUATTRO

ACE-QUATTRO has:

- Standard FFT, Synthetic 1/3 Octave standard,
- Quality Control, Point & Direction,
- Sound Power, Sound Intensity,
- Acoustic Intensity, Human Vibration,
- Sound Quality, Demodulation,
- Disk Record & Playback Analysis,
- Frequency Domain Compensation,
- Real Time Octave Analysis, Event Capture,
- 4-32 Inputs (Abacus), 2-8 Outputs + Tachy,
- ActiveX command & control macro programs,
- Single to Multi-Plane Balancing ...and more

A new Sound Level Meter!

from BSWA

BSWA 308 has:

IEC 61672 Class 1
JJG Class 1
SPL, LEQ, Peak,
Max, Min
A, C, Linear
Fast Slow Impulse
29 dBA~131 dBa
20 Hz ~20 kHz
DR:- 102 dB
IEPE, TNC connect
160 x 160 LCD
4 AA batteries
300x70x36 mm
~ 620 grams

A low cost Class 1 intergrating sound level meter featuring an industrial designed housing and a high level of comfort and style. Capable of measuring 3 parameters simultaneously with A, C & Z frequency and 1 time weighting. Also the equivalent continuous sound pressure level max & min values. An ideal instrument for general noise measurements

BSWA TECH

MEASUREMENT MICROPHONES.

microphones & accessories for Australian & NZ.

High quality, calibrated electret prepolarized microphones to class 1 & 2 & preamplifiers.

Some of the Accessories available:

- IEPE power sources, - portable sound level calibrators,
- USB powered 2 channel measurement soundcard
- a 12 speaker dodecahedral sound source,
- compact light weight 2 channel power amplifiers,
- a self contained Tapping Machine sound source for foot fall measurements.
- impedance tubes providing 125 Hz to 3200 Hz range,
- Outdoor noise monitoring, terminal and software
- Small Reverberation chamber,
- Artificial Ear, Mouth & Head

Closed Loop Random Acoustic Control.

SignalStar Matrix Random Acoustic Control software provides precise, real-time, control of reverberant acoustic chambers.

The DP Random Acoustic Control software is designed to simulate high intensity acoustic noise such as that experienced during a rocket launch. The Random Acoustic Control software runs on the Data Physics ABACUS DSP system platform which is ideally suited for closed loop acoustic control and testing. ABACUS provides >120 dB of control dynamic range with excellent channel to channel phase match, necessary for accurate control of reverberant acoustic chambers. ABACUS also provides 32 input channels and up to 8 output channels. With high dynamic range, the separate output channels can be used to drive acoustic exciters in different frequency ranges. Random Acoustic control includes test profiles with 1/1 octave, 1/3 octave and narrowband control. Alarms and aborts may also be defined based on the overall SPL level.

AAS 07/10

For more information phone: **02 9975 3272**
visit: ***www.kingdom.com.au***
or mail: ***kingdom9@kingdom.com.au***

KINGDOM PTY LTD
Phone 02 9975 3272

New Zealand Acoustics

Volume 25, 2012 4th Quarter

Features

Regulars

Cover Image: Neuron, Copyright © 2003 Nicolas P. Rougier

Source: Wikipedia Commons: http:// http://commons.wikimedia.org/wiki/File:Neuron-SEM-2.png

New Zealand Acoustics is published by the Acoustical Society of New Zealand Incorporated, PO Box 1181, Auckland, and is delivered free of charge.

Contributions to the Journal are encouraged, and may be sent directly to the Editor either by email, or by post c/o the Acoustical Society of New Zealand Incorporated, PO Box 1181, Auckland.

From the President and Editor

From the President

Dear Members,

One of the funny things about life is how all the clichés are true.

This annoys me somewhat, especially when I'm trying to explain what it's like to be a dad to someone (who isn't). In these situations I'd like to say something really pithy, unique and relevant... so that they'll get it. Y'know... really get it. But no matter what I say on the subject, it always sounds like I'm quoting from a blimmin' Hallmark Card. "It's the most difficult but the most rewarding thing"... "It's a rollercoaster ride that you can't get off"... gumpf like that.

It's the same thing at this time of year. I'd like to say something really significant about how unbelievably quickly 2012 has flown past. How New Year's Eve 2011 only seems like a month ago. But everyone I've talked to is saying the same thing (and I bet you're thinking it)... so best to just keep quiet and move on with my column. Gee look at that, I'm three paragraphs in already. How time flies...

This is my second column as president. Since my first column, we have witnessed a significant event in the history of NZ acoustics: On 21 November 2012, Dr Mark Poletti (ASNZ Council Member) was honoured by The Royal Society. He was awarded The Cooper Medal for 'research in physics or engineering' for his world-leading development on assisted reverberation systems for concert hall acoustics.

His system (now called 'Constellation', and marketed worldwide by Meyer Sound) is revolutionising concert

halls around the world by providing the ability to vary reverberation time at the touch of a button. And believe it or not, the Aotea Centre now has a Constellation system installed. I'm very keen to organise an ASNZ branch

Publication Dates and Deadlines

New Zealand Acoustics is published quarterly in March, June, September, and December.

The Deadline for material for inclusion in the journal is 1st of each publication month, although long articles should ideally be received at least 2 weeks prior to this.

Advertising

Enquiries regarding advertising are welcome. For a list of current prices please contact the advertising manager: fadia.sami@earcon.co.nz or phone 09 443 6410 or fax 09 443 6415

Society Membership

Associate Membership of the Acoustical Society of New Zealand is open to anybody interested in acoustics.
Members receive benefits including;

- Direct notification of upcoming local events
- Regular mailing of Noise News International
- Reduced charges for local and national Society events
- Priority space allocation for trade stands at society events
- Discounted rates on selected acoustic products

To join the society, visit www.acoustics.ac.nz or contact the Secretary.

meeting next year once the calibration of the system is complete. We'll fly Mark up for the occasion so we can be introduced to Constellation by the man himself. Exciting stuff!

Since the last journal issue the ASNZ council has held one meeting and I can say that things are ticking along nicely. Our primary focuses at the moment are finalising our proposal for a Continued Professional Development (CPD) framework, building membership, and (to facilitate this) working on expanding the list of benefits one receives by being a member/affiliate. I just know that there are people out there (both in NZ and abroad) for whom the ASNZ would hold some interest, and I aim to continue reaching out to these people. It's just a matter of finding the best way. I welcome comments and suggestions from members on this issue.

Members may be pleased to hear that our Café and Restaurant Acoustic Index (CRAI) system has sparked some interest overseas. In the last month we have been contacted by two groups (one in UK, the other in Australia) applauding our initiative and asking for collaboration in setting up similar systems in those countries. Congratulations to Stuart Camp for keeping CRAI going and I look forward to seeing its future developments in NZ and abroad.

Finally, I'd like to update you on the status of the Christchurch Town Hall, which sustained significant damage in the February 2011 earthquake. For those who may not know, this is a space with world renowned acoustics – the first hall designed by Sir Harold Marshall utilising his novel theories on lateral fraction. On 22 November this year, Christchurch city councillors voted unanimously to rebuild it at a cost of $127 million... however Earthquake Recovery Minister Gerry Brownlee could still veto this decision. He'd better not. I can write a pretty shirty letter when the need arises.

And on that optimistic note, I wish you all a very happy and safe Christmas and a Happy New Year. See you in 2013 (unlucky for some, but not for us!), and enjoy this issue of New Zealand Acoustics!

Yours faithfully,

James Whitlock

Editor's Ramble

Dear Readers,

By the time you read this I hope you are enjoying (or have enjoyed) the delights of the festive season and maybe some sunny weather.

Our family will spend some time this summer camping in an attempt to share with my kids the same kind of holidays I remember. We'll be staying in tents at holiday park near the beach. It will be crowded and I suspect I am going to spend many hours awake at night pondering the acoustic insulation properties of canvas!

This issue celebrates some of the best of the recent conference in Wellington, with three papers reprinted for your interest.

The first concerns the physiological responses to noise. This paper was delivered in an excellent presentation by Jenny Lee at the conference, for which she was awarded the prize for best student presentation.

The second article is from IRL in Wellington and includes work from Mark Poletti. As James has previously mentioned, Mark has recently been awarded the prestigious Cooper Medal and I hope we will feature more about this in the next issue. The paper concerns an efficient method for simulating high order sources in a reverberant room. The work is quite mathematical and it has taken me considerable time to format the expressions. As usual, any mistakes that have occurred in the equations are my own.

The final piece of research is about using mixtures of granular mixtures of materials for floor toppings of timber framed floor systems. This work comes from Scion with Grant Emms as the author and presents some new experimental results.

As usual, the rest of the journal contains a new crossword, some snippets about acoustics in the news and a product announcement. Enjoy!

All the best for the new year,

John Cater ¶

Neural Correlates of Noise Annoyance and Sensitivity

Jenny S.Y. Lee[1], Michael J. Hautus[1] and Daniel Shepherd[2]

[1]**Department of Psychology, The University of Auckland, New Zealand**

[2]**Department of Psychology, Auckland University of Technology, New Zealand**

This paper was previously awarded best student presentation at the 21st Biennial ASNZ Conference, Wellington, NZ

Abstract

The relationship between noise and affective response is not well understood, and there have been calls for further physiological investigation. To investigate subjective responses to noise, an attempt is made here to analyze the auto-correlation function of alpha activity during the presentation of annoying sounds. Twelve real-world sounds (e.g. baby's cry, snoring) were presented to a small sample (n = 16), who listened while having their scalp potentials recorded. Noise sensitivity questionnaires were used to assess participants' sensitivity to noise in general. Findings indicate that those who are noise sensitive appear easily aroused by noise regardless of the magnitude of annoyance. In contrast, participants who classified as noise resistant are typically aroused only when the most annoying sounds are presented. Theses result suggests a difference in processing between the noise sensitive and the noise resistant individuals. The current investigation may provide a basis for future studies to evaluate the underlying neural processes associated with noise annoyance.

INTRODUCTION

At the psychological level of description, noise can be broadly defined as unwanted and intrusive sounds that one would prefer not to hear [1]. Noise interferes with daily activities and these disturbances often elicit feelings of annoyance or irritations in the listener [2]. People who are extremely annoyed by noise may experience maladaptive, negative emotions such as anger or fear towards the source of noise [3]. These emotions are usually accompanied by physiological arousal, which could further reinforce the initial affective reactions. Noise annoyance describes a multifaceted response that covers both affective dimensions and the immediate behavioural effect of noise [4].

An increasing body of literature supporting the role of noise sensitivity in noise perception is emerging [5].

Noise sensitivity is defined as a mediating factor between noise-induced annoyance and noise exposure [6]. Weinstein [7] postulated that noise sensitivity could be understood as a general tendency of the individual to express negative judgments of their immediate environment. Stansfeld [1] further refined this definition to consider noise sensitivity as a stable personality trait composed of two key characteristics. First, noise sensitive individuals have a predisposition to attend to sounds and to perceive them negatively. Second, these individuals display stronger emotional reactions to noise [1].

Unfortunately, most investigations into noise impacts mainly focus on annoyance generated by noise from transport infrastructures and industrial complexes. Comparatively, other noises such as the rustling of papers, snoring or a baby's cry have often been neglected [8]. To date, the effects of these everyday sounds remained inconclusive. Accordingly, a broader approach in measuring noise annoyance is needed.

In the past decade, a neural-based model has been developed by Ando [9] to assess subjective preferences for sounds. According to this model, subjective preference is mirrored in changes in alpha activity when exposed to noise [10]. This model takes advantage of the physical properties of sound waves to calculate how the brain processes acoustic information at each stage of the auditory system.

Numerous studies by Ando [10] calculated the persistence of alpha activity in the electroencephalogram (EEG) using autocorrelate functions (ACF). The ACF is a procedure for identifying the similarity within a monaural signal as a function of time-lag [11]; that is to find repeating patterns within the signal itself across time. Therefore, the continuity of alpha activity describes how self-similar the signal is within a set period of time.

Interestingly, it has been found that the effective duration of temporal and spatial factors of sounds are processed differently in the brain. The effective duration is the time over which the sound is acoustically self-similar and less degraded by other factors before it enters the ears [10]. Hence, this represents the short period of time where the properties of sounds remain the same.

A study by Mouri, Akiyama and Ando [12] found a correlation between the effective duration of sounds and that of alpha wave activity with different subjective preferences. Participants were asked to listen to 10 seconds of music inside an anechoic chamber while having electrical activity recorded from their scalps [10]. Both the neural activity and the sound stimuli were analysed using the ACF. The effective duration of alpha waves in the left hemisphere persistently correlated with the effective

duration of (and thus preference for) the 10 second piece of music [12]. This investigation revealed two important pieces of information regarding the auditory-brain model. First, the persistence of alpha waves suggests a preference for that sound stimulus. [12]. Second, greater alpha waves were found in the left hemisphere compared to the right suggesting that the left hemisphere is more responsive to positive evaluations of sounds.

Another study by Soeta, Nakagawa, Tonoike and Ando [13] explored different patterns of neural activity in participants listening to different sounds. The sound stimuli included pure tones or bandpass noises with a centre frequency of 1000 Hz. Participants were required to listen to these sounds via an earpiece within an anechoic chamber [13]. Results revealed that alpha activity was detected in the left hemisphere during pure tone conditions [13]. However, during the presentation of bandpass noise, the effective duration of the alpha rhythm decreased dramatically. These findings were consistent across participants in the study suggesting that annoyance could be a function of the persistence of brain oscillations.

The primary intention of the present investigation was to develop a quantitative procedure to guide future studies in the assessment of noise annoyance. Specifically, to quantify the qualitative aspects of noise annoyance by comparing the corresponding changes in alpha persistence when annoying stimuli were presented. Furthermore, these changes will also be compared against the listeners' level of noise sensitivity. The aforementioned studies of the auditory-brain model suggested that subjective preference for a sound could be recognized from the increase of alpha persistence. Consequently, it is postulated that alpha persistence would decrease when annoying acoustic stimuli are presented irrespective of the level of sensitivity.

MATERIALS AND METHODS

Participants

The present study consisted of 17 participants (7 male), aged between 18 and 28 years (mean age = 22.37 years). Data from one participant was discarded prior to analysis due to inattention during the session. Participants were categorised into two groups; noise sensitive and noise resistant, based on their scores from the Noise Sensitivity Questionnaire (NOISEQ). Each group consisted of eight participants. None of the participants reported any forms of hearing impairment or a medical history of neurological disease. Ethics approval was obtained prior to the commencement of the study, as well as informed consent from each participant.

Stimuli and apparatus

Acoustic stimuli

A total of 12 digitized emotional sounds taken from the International Affective Digitized Sounds (IADS) library were used [14]. The duration of each sound was six seconds. The 12 stimuli were selected based on their mean valence and arousal scores as reported by Redondo, Fraga, Padron and Pineiro [15]. Stimuli were presented using LabView (TM) software (National Instrument; NI). The level of the stimuli was adjusted using programmable attenuators (Tucker-Davis Technologies; TDT), to yield 70dB SPL at the earphone. The stimuli were then routed through a headphone driver (TDT HB7) and presented via inserted earphones (Etymotic ER2).

Electroencephalogram (EEG)

All EEG recordings were conducted in a modular shielded room using 128-channel Ag/AgCl electrode nets (Electrical Geodesics Inc.), according to the 10/20 international system of electrode placement. All EEG signals were recorded continuously at a sampling rate of 250 Hz (0.1-100 Hz analogue bandpass) with Electrical Geodesics Inc. amplifiers (200 MΩ input impedance). Electrode impedances were kept below 40 kΩ. All EEG signals were acquired using a common vertex (Cz) reference and were processed by Net Station (Version 4.2) on an 8-core Apple Mac Pro workstation.

Each session was divided into two blocks. A total of 12 different sound stimuli were presented to the listener: each stimulus was repeated 7 times in each block. Thus a total of 168 sounds (12 x14) were presented to the listener in one experimental session. The order of stimuli presentation was randomized and the interstimulus (offset to onset) interval was 6000 ms.

Noise sensitivity questionnaire (NOISEQ)

Each participant's level of noise sensitivity was estimated using the Noise Sensitivity Questionnaire (NOISEQ), which was adopted from the Weinstein Sensitivity Scale. The scale consists of 35 items which when averaged provide a measure for global noise sensitivity, as-well-as sensitivity in five everyday life domains (leisure, work, habituation, communication and sleep). Each item asks the participant to identify their level of agreement regarding noise-related statements on a five point Likert-type scale. Global noise sensitive scores were computed as the mean of 35 items on the scale. Low scores indicate greater sensitivity whereas higher scores represent greater resistance to noise.

Annoyance ratings

The degree of perceived annoyance for each sound stimulus was recorded on a computer immediately after each stimulus was presented. During the annoyance rating section, the same 12 sound stimuli were presented consecutively to the listener in an anechoic chamber. After the presentation of each sound stimulus, participants were asked to rate, on a scale of 1 (least annoying) to 5 (most annoying), the degree to which the sounds were annoying. The presentation order of stimuli was randomized.

Procedure

The study was conducted within a laboratory setting, including the completion of the Noise Sensitivity Questionnaire prior to the experiment.

The experiment was divided into two parts: EEG recordings and annoyance ratings. The EEG section was divided into two blocks and participants were given a short break (5-10 minutes) between them. During each block, participants sat 57 cm in front of a computer monitor in a modular shielded room and listen to sounds. Participants were instructed to sit still and listen to the sounds passively while having their scalp activity measured. Neutral pictures, such as tables and chairs, were shown on the monitor as the sound stimuli were presented. Each block was approximately 15 minutes in duration.

After the EEG recordings, participants were seated comfortably

in an anechoic chamber while they rated the degree of annoyance for each sound stimulus. The same series of sounds were presented in random order. Each participant was instructed to attend passively to the sounds and imagine hearing those sounds when they were concentrating on a task. The entire annoyance rating procedure was approximately 20 minutes. All experimental procedures were completed individually, and no incentives were offered.

Data analysis

All statistical analyses, parametric, non-parametric, and autocorrelation, were conducted using the Statistical Package for Social Science (SPSS) version 17.

EEG analyses

After completion of data collection, EEG raw files were filtered with a Butterworth band-pass filter (alpha; 8Hz-12Hz) and segmented, according to event markers, into 6000-ms epochs, including a 100-ms pre-stimulus baseline. Ocular artefacts were removed, and trials in which any of the electroculogram channels were marked as non-responsive were discarded prior to the averaging process. The voltages measured from these electrodes were averaged in their respective sound stimuli condition and a grand average was calculated for each members of the noise sensitive and the noise resistant group. The autocorrelation functions for all grand averages were computed, and the average autocorrelation from time zero were calculated according to level of sensitivity and 600-ms pre- and post-stimlus onset.

Noise sensitivity questionnaires and annoyance ratings

Prior to computing the noise sensitivity scores, any negatively-worded items were recorded, and means and standard deviations calculated and inspected for evidence of floor or ceiling effects.

Participants were divided into groups of noise sensitive and noise resistant according to the median score. Participants' annoyance ratings were computed and a total value of annoyance was calculated for each sound stimulus. Sound stimuli were ranked from most annoying (highest ratings) to least annoying (lowest ratings) for both the noise sensitive and noise resistant participants. Thus, in this way, the 6 most annoying and the 6 least annoying sound stimuli were identified.

RESULTS

Study Population Characteristics

Independent-samples t-tests were conducted to compare the noise sensitivity scores and age between the noise sensitive and the noise resistant participants (see Table 1).

Table 1. Descriptive data for the study population. Re-sults were presented in means (s.d).

	Noise sensitive (n=8)	Noise resistant (n=8)	Study total (n=16)
Age	23.00 (2.32)	21.75 (3.45)	22.37 (2.92)
Noise sensitivity scores	2.55 (0.22)	3.22 (0.32)	2.88 (0.44)

Table 2. Ratings for each sound stimulus in descending order of annoyance for the noise sensitive and the noise resistant individuals.

Degree of annoyance	Noise sensitive	Noise resistant
Most annoying	Mosquito	Baby crying
	Snoring	Snoring
	Baby crying	Mosquito
	Lawnmower	Chewing
	Chewing	Lawnmower
	Radio tuning	Radio tuning
	Whistling	Jet take-off
	Seagull	Toilet flushing
	People laughing	Whistling
	Dog barking	People laughing
	Toilet flushing	Dog barking
Least annoying	Jet take-off	Seagull

There was a significant difference in sensitivity scores between both groups ($t(14) = -4.88$, $p < .001$). However, the effects of age did not reach statistical significance. Furthermore, chi-square tests (Yates Continuity Correlation) indicated no significant association between gender and level of sensitivity ($X^2(1, n = 16) = 2.4$, $p = .12$, phi = -0.52).

Annoyance Ratings

The annoyance ratings for all sound stimuli were computed and ranked from the highest score (most annoying) to the lowest score (least annoying) for both groups. As shown on Table 2, the most and least annoying sound stimuli were the same for both the noise sensitive and the noise resistant participants.

Autocorrelation Functions of Alpha Persistence

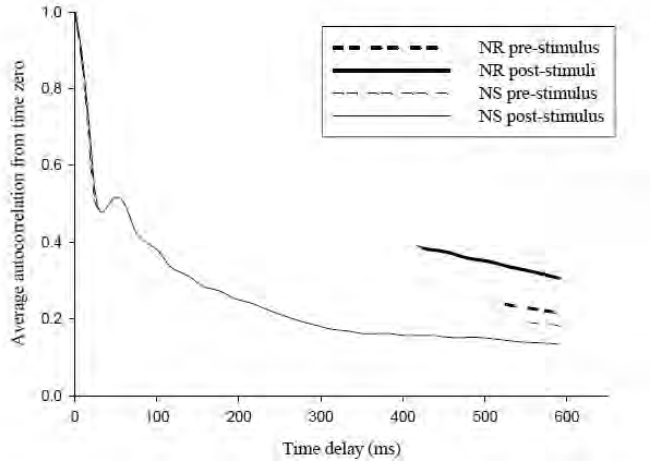

Figure 1. Alpha persistence for the pre- and poststimulus onset between the noise sensitive (NS) and noise the resistant (NR) participants.

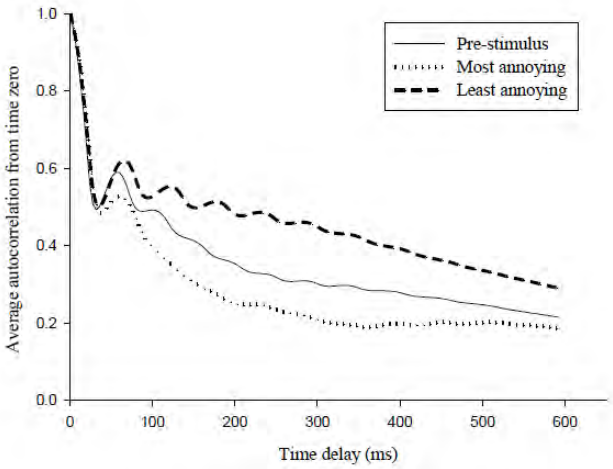

Figure 2. Alpha persistence for pre-stimulus, the most and the least annoying post-stimulus conditions for the noise resistant participant.

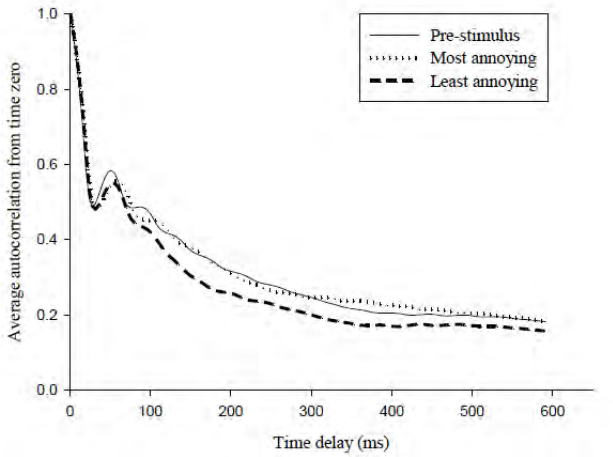

Figure 3. Alpha persistence for pre-stimulus, the most and the least annoying post-stimulus conditions for the noise sensitive participants.

Pre- and Post-stimulus Onset

Overall, there were marked changes in alpha persistence after the stimuli were presented. In particular, presentation of the stimuli led to an increase in alpha persistence for the noise resistant participants as shown in Figure 1. In contrast, a decrease in alpha persistence was observed upon the presentation of the stimuli for the noise sensitive participants.

Close inspection revealed a dramatic difference in alpha persistence among levels of annoyance between members of the noise sensitive and the noise resistant group. As shown in Figure 2, compared to the persistence prior to stimulus presentation, the most annoying stimuli resulted in a decrease in alpha persistence for the noise resistant participants. Conversely, the least annoying stimuli were found to increase the persistence in alpha activity in this group.

Meanwhile, the changes in alpha persistence were less apparent for members of the noise sensitive group. As shown in Figure 3, compared to the alpha persistence before the onset of stimuli, the least annoying stimuli demonstrated a decrease in alpha persistence. Remarkably, the alpha persistence before and after the presentation of most annoying stimuli were relatively similar.

DISCUSSION

In the current investigation, the subjective evaluation of noise between noise sensitive and the noise resistant individuals was examined. The primary intention of the present study was to ascertain whether changes in phased-locked alpha persistence could be used as an objective indicator for assessing noise annoyance.

Building from the work of Ando [10], the autocorrelation

When you need a little peace and quiet, just close the door.

Pacific Door Systems' new 'AD' series single-leaf acoustic doorsets let you mix and match sizes of vision panels, frame types and door surfaces while still achieving acceptable STC/Rw ratings.

These flush-panel doors, hung in timber or steel frames, are the result of 15 months of intensive testing and development in our own in-house acoustic laboratory—a two-chamber facility designed by a leading Acoustic Engineering Consultancy to test full size products in accordance with ISO 140-1 and 3, using Norsonic microphones and sound level meter, and Norbuild software.

Each door in our new range is individually certified to meet both international standards and your specifications.

Lightweight AD100. Interior doorset for general use, offers STC/Rw 35. Priced to compete with solid core doors and proprietry seals having a lesser rating.

Medium-Weight AD200. Interior doorset offering up to STC/Rw 36–38, which can also be incorporated into the PDS 'hospital series' or become a commercial-quality exterior unit rated to STC/Rw 40.

Medium-Weight AD300. Robust interior doorset achieving 40 STC/Rw. Can be incorporated into the PDS 'hospital series.' Bridges the commercial cost gap between AD200 and AD400.

Medium-Weight AD400. The 'Flagship' of our range. Robust interior doorset offering STC/Rw 43 for any environment.

In late 2012 we'll release 'AD' series pairs, a new fire/acoustic single and pair unit, and a 50 plus STC/Rw sound attenuation unit.

For full specifications of our range of acoustic doors and other products, visit www.pacificdoors.co.nz

17 Meachen Street, Seaview, Lower Hutt.
Tel: (04) 568 6109; Fax: (04) 568 8531; Email: sales@pacificdoors.co.nz
For specifications, visit **www.pacificdoors.co.nz**

Pacific Door Systems Limited

MMA 12/3

function was applied to analyse the duration of alpha activity when stimuli with differences in annoyance were presented. Accordingly, differences in the persistence of alpha activity between noise sensitive and noise resistant individuals could validate the effectiveness of using the autocorrelation function to assess the subjective evaluation of annoying sounds. To date, the precise physiological and functional role of alpha activity remains controversial. The classical understanding of alpha rhythms suggests that they are associated with a state of mental and physical relaxation [16].

High alpha oscillations are found during meditation and have shown to be inversely correlated with arousal level [17]. In contrast, low alpha oscillations are correlated with increased attention or other forms of mental processing [18]. These findings suggested that the individual with high alpha activity could be in a state of tranquillity and free of mental activity.

Moreover, existing research suggests that alpha rhythms represent a stand-by state of the brain [19]. To illustrate, the idle state of the brain could be thought of as similar to a computer that is merely turned on. As the lights on a computer could act as an indicator for its activation, alpha oscillations could also be a marker for this activated state. Some studies suggest that during this state, alpha oscillations have inhibitory control over other mental processing [20]. Thus decrease in alpha persistence would be an indicator for the activations of networks of neurons to carry out oriented functions [19].

The reduction in phase-locked alpha persistence demonstrated in the present study suggests that extremely annoying sounds can induce alpha desynchronization in both noise sensitive and noise resistant individuals (see Figure 2 and 3). These results are consistent with studies by Soeta et al [13] where a reduction of alpha activity was observed when bandpass noises are presented to participants.

A disruption in alpha oscillation suggests that the individual is no longer at a state of relaxation and other mental processing may be occurring [19]. This implication is rooted in numerous psychophysiological studies where diminished alpha rhythms have been observed during motor activation [21], attention processing [22], and sensory-semantic processing [23]. Therefore, it is plausible that a lowering of alpha persistence after the presentation of sounds is due to arousal and activation in mental functioning.

Speculatively, the increase of alpha persistence after the least annoying sounds are presented to the members of the noise resistant group (see Figure 2) may reflect the strengthening of the inhibitory function of the alpha rhythm. The aforementioned studies have illustrated that attention and other mental effort is reflected in a reduction in alpha activity, thus an increase in alpha rhythm will indicate a lack of mental processing in the cortex [17]. This proposes that the noise resistant participants in the present study may have the capacity to filter out noises that are judged as less annoying.

In addition, the least annoying sound results in a lower alpha persistence compared to the most annoying sounds for the noise sensitive participants (see Figure 3). Admittedly, this finding appears contradictory to what is discussed so far given that the most annoying sounds are expected to decrease alpha persistence. Yet it is possible that large variability between members of the noise sensitive group may have lead to this result.

To illustrate, participants in the present study were categorize into noise sensitive and noise resistant based on their total noise sensitivity score relative to the sample' median score. Thus it is reasonable to suspect that large individual differences among noise sensitive participants may have led to this mixed finding. Moreover, measures of noise sensitivity among participants were relatively low compared to field studies. For example, an extensive airport study by Shepherd, Welch, Dirks and Mathews [24] had a mean sensitivity score of 3.50. This value is greater compared to the mean sensitivity score of 2.88 found in the present study. Therefore, differences in the level of sensitivity may have contributed to the inconsistent results among noise sensitive participants. In short, the reduction of alpha persistence between the noise sensitive and the noise resistant participants may reflect arousal and activation of other mental processes.

Moreover, the generation of alpha activity in noise resistant participants when annoying sounds are presented suggests differences in processing. As the decrease of alpha persistence was only found when the most annoying sounds were presented, this implies an ability to differentiate between magnitudes of annoyance using electrophysiological indices.

CONCLUSION

In the past decades, increases in community noises have been concerning the general population. As noises from transport infrastructures and industrial complexes becomes a daily nuisance, constant exposure becomes a psychological and physiological burden.

Past approaches to the assessment of noise annoyance relied on correlating levels of annoyance with acoustic and non-acoustic properties of noise. Among these non-acoustic parameters of noise, an individuals' level of sensitivity to noise has been shown to influence self-reported annoyance. With the advanced neuroimaging technologies, a better understand of individual differences in noise annoyance is possible.

In the present study, the persistence of alpha activity provides a promising approach to understand the qualitative aspects of noise annoyance. Compared to traditional methods, a description of noise annoyance is obtained by studying the durations of alpha activity among individuals with different levels of noise sensitivity. The differences in alpha persistence between the noise sensitive and the noise resistant participants provided information on how annoying sounds are perceived.

Specifically, the noise sensitive participants have a tendency to be aroused by noise easily. They also have difficulties in distinguishing noises that are different in magnitudes of annoyance. In contrast, being insensitive to noise is shown to have a buffer effect. It protects the noise resistant individuals from being distracted by noises that are judged as less annoying. However, as the precise functional role of alpha activity remains inconclusive, evidence from the present study may need to be interpreted with cautions. Irrespective, the current investigation provides supporting evidence suggesting that alpha persistence could be used to understand the subjective evaluation of sounds.

IMPLICATIONS

With respect to the objectives of the present investigation, the findings revealed here show that the persistence of alpha activity, as shown by the autocorrelation function, may be an objective tool for assessing noise annoyance. This additional tool could add to the current understanding regarding sensitivity to noise from a neurological standpoint. Results from the current study confirm that the characteristics of noise sensitive participants may be rooted in physiology. For instance, a tendency to be aroused by noise is evident among noise sensitive participants. Moreover, the characteristics of noise resistant participants, such as the apparent protective effect against noise are evident in the present study. Taken together, findings from the current investigation reiterates how vital an objective measurement is for noise annoyance assessment.

ACKNOWLEDGEMENTS

The authors would like to thank Ms. Veema Lodhia for her assistance in data analysis.

REFERENCES

[1] Stansfeld, S. A. (1992). Noise, noise sensitivity and psychiatric disorder: epidemiological and psychophysiological studies. Psychological medicine. Monograph Supplement, 22, 1-44.

[2] Bluhm, G. L., Bergling, N., Nordling, E., & Rosenlund, M. (2011). Road traffic noise and hypertension. Occupational and environmental medicine, 64(2), 122-126. Doi:10.1136/oem.2005.025866.

[3] Vastfjall, D. (2002). Influences of current mood and noise sensitivity on judgements of noise annoyance. The journal of psychology, 136(4), 357-370.

[4] Rylander, R. (2004) Physiological aspects of noise-induced stress and annoyance. Journal of sound and vibration,277(3),471-478. Doi:10.1016/j.jsv.2004.03.008

[5] Heinonen-Guzejev, M. (2009). Noise sensitivity- medical, psychological and genetic aspects (Doctorial dissertation). University of Helsinki, Finland.

[6] Ellermeier, W., Eigenstetter, M., & Zimmer, K. (2001). Psychoacoustic correlates of individual noise sensitivity. Acoustical society of America, 109(4), 1464-1473. Doi:10.1121/1.1350402.

[7] Weinstein, N. D. (1978). Individual differences in reactions to noise: a longitudinal study in college dormitory. Journal of applied psychology, 63(4), 458-466.

[8] Stansfeld, S. A. (1992). Noise, noise sensitivity and psychiatric disorder: epidemiological and psychophysiological studies. Psychological medicine. Monograph Supplement, 22, 1-44.

[9] Ando, Y. (1983). Calculation of subjective preferences at each seat in a concert hall. J. Acoustical society of America, 74(3), 873-887.

[10] Ando, Y. (2009). Auditory and visual sensations. New York: Springer.

[11] Brazier, M. A. B., & Casby, J. U. (1952). Crosscorrelation and autocorrelation studies of electro-encephalogrphic potentials. Electroencephy and Clinical neurophysiology,4,201-211. Doi:10.1016/0034694(52)90010-2.

[12] Mouri, K., Akiyama, K., &Ando, Y. (2000). Relationship between subjective preference and the alpha-brain wave in relation to the initial time delay gap with vocal music. J. Sound and Vibration, 232(1), 139-147. Doi: 10.1006/jsvi.1999.2689.

[13] Soeta, Y., Nakagawa, S., Tonoike, M., & Ando, Y. (2004). Magnetoencephalographic responses correspond to individual annoyance of bandpass noise. Journal of Sound and Vibration, 277(2), 479-489. Doi: 10.1016/j.jsv.2004.03.009.

[14] Bradley, M. M., & Lang, P.J. (2000) Affective reactions to acoustic stimuli. Psychophysiology, 37, 204-215.

[15] Redondo, J., Fraga, I., Padron, I., & Pineiro, A. (2008).Affective ratings of sound stimuli. Behavior researchmethods,40(3),784-790.Doi: 10.3758/BRM.40.3.784.\

[16] Goldman, R. I., Stern, J. M., Jr, J. E., & Cohen, M. S. (2002). Simultaneous EEG and fMRI of the alpha rhythm.BrainImaging,13(18),2487-2492. Doi:10.1079/01.wnr.0000047685.08940.d0.

[17] Barry, R. J.,Clarke, A. R., Johnstone, S. J., Magee, C. A., & Rushby, J. A. (2007). EEG differences between eyes-closed and eyes-open resting conditions. Clinical neurophysiology, 118(12), 2765-2773. Doi: 10.1016/j.clinph.2007.07.028.

[18] Laufs, H., Kleinschmidt, A., Beyerle, A., Eger, E., Salek-Haddadi, A., Preibisch, C., et al. (2003). EEG-correlated fMRI of human alpha activity. Neuroimage, 19(4),1463-1472. Doi: 10.1016/S1053-8119(03)00286-6.

[19] Bed-Simon, E., Podlipsky, I., Arieli, A., Zhdanov, A., & Hendler, T. (2008). Never Resting Brain: simultaneous representation of two alpha related processes in humans. PLoSONE,3(12),e3984. Doi:10.1371/journal.pone.0003984.

[20] Liley, D. T. J., Bojak, I., Dafilis, M. P., Veen, L. V., Frasoli, F., & Foster, B. L. (2011). Bifurcations and state changes in the human alpha rhythm: theory and experiment, In D.A. Steyn-Ross & M. Steyn-Ross (Eds.), Modeling phase transitions in the brain, NY: Springer. Doi: 10.1007/978-1-4419-0796-7-6.

[21] Niedermeyer, E. (1997). Alpha rhythms as physiological and abnormal phenomena. International Journalofpsychophysiology,26(1-3),31-49.Doi:10.1016/S10678760(97)00754-x.

[22] Klimesch, W., Doppelmayr, M., Russegger, H., Pachinger, T., & Schwaiger, J. (1998). Induced alpha band power changes in the human EEG and attention. Neuroscience Letters, 244(2), 73-76. Doi: 10.1016/S0304-3940(98)00122-0.

[23] Schurmann, M., & Basar, E. (2001). Functional aspects of alpha oscillations in the EEG. International Journal of psychophysiology, 39(2-3), 151-158. Doi: 10.1016/S10678760(00)00138-0.

[24] Shepherd, D., Welch, D., Dirks, K. N., & Mathews, R. (2010). Exploring the relationship between noise sensitivity, annoyance and health-related quality of life in a sample of adults exposed to environmental noise. International Journal of Environmental Research and Public Health, 7(10), 3579-3594. Doi: 10.3390/ijerph7103580. ¶

Sound Field of a Directional Source in a Reverberant Room

Terence Betlehem and Mark Poletti

Industrial Research Limited, 69 Gracefield Road, Lower Hutt

This paper was previously presented at the 21st Biennial ASNZ Conference, Wellington, NZ

Abstract

It is useful to have an efficient method to determine the sound field in a room produced by a source that is not omnidirectional. A method is thus developed for simulating a "higher order" source with an arbitrary directional pattern in a reverberant room. Several types of directional sources are subsumed by the higher order source, including an arbitrarily vibrating cylinder and an array of vertical line sources arranged on a cylinder. The sound field is calculated by extending the image-source method. For simplicity the sound is modelled in 2-D where sources are either tall or have an infinite vertical extent. A modal expansion of the sound field is used, which reduces the computation of calculating the sound field over a large number of points. The method is particularly suited to array signal processing where the sound field is sampled at multiple points. Efficient algorithms are presented for simulating both circularly-shaped regions absent of sound sources and the entire room.

INTRODUCTION

It is common in room acoustics to simulate the sound field of the omnidirectional source. Yet realistic sources are directional. When the size of a sound source is large in comparison to the acoustic wavelength, it typically creates sound which varies in intensity from one direction to another. Above bass frequencies electrodynamic loudspeakers are directional.

Many sound sources, such as musical instruments also exhibit a natural directivity [1, ch. 4]. It is of advantage in sound reproduction applications to use loudspeakers with directional characteristics. Sound can be directed for example using dipoles [2] towards the walls to generate room reverberation and create a feeling of ambience, or directed toward the listener using cardioid loudspeakers to create a clearly localisable phantom source. In this paper, an efficient method is proposed for simulating the sound field of a directional source in a room.

Accurate methods of simulating a sound field are based upon the wave equation. Many of these methods work by dividing either the free-space or surfaces of the room into elements. Finite difference time domain (FDTD) methods approximate the time domain wave equation over a spatial grid with a difference equation, a number of which are summarized in [3].

Unfortunately the accuracy suffers from numerical dispersion. The wave equation can also be converted into an integral equation and solved with either the finite element method (FEM) or boundary element method (BEM) [4, 5]. The advantage of element methods over FDTD is that elements can be more densely positioned around intricate geometrical structures like the human pinna [6]. The equivalent source method (ESM) [7], where the scattering environment is replaced with an equivalent set of sources, can also account for cylinder scattering and non-regular room geometries. Each of these methods can be adapted for directional sources in a room by imposing a boundary condition on sound velocity on the surface of the directional source.

An efficient sound field model for the omnidirectional source in a rectangular room is the image-source method [8]. Fractional delay filters were used in [9] to permit a time-domain implementation. In [10], the speed of computation of an acoustic transfer function has been improved by replacing the late reverberant tail, which requires computing thousands of image-sources, with a decaying diffuse noise term. Unfortunately this method fails to account for the correlation in the reverberant tail for closely sampled locations. It is unsuitable for array signal processing applications for which the tail holds relevance.

A more promising method is that of [11], where a multipole expansion was exploited to reduce the computational requirements. A simulator for directional sound sources in the room was implemented by modelling a source using its farfield directivity pattern [12]. However this does not account for the variation of the directivity pattern in the nearfield with distance.

This paper presents an extension of the image-source method to an arbitrary directional source in a 2-D rectangular room. The method is accurate in simulating the soundfield in a room with multiple numbers of vibrating cylinders. A frequency-domain method is presented, where the soundfield can be determined discretely at a number of frequencies. Time-domain simulations over a band of frequency can also be performed by sampling the soundfield at adequate numbers of frequencies.

An outline of the paper is as follows. The original image-source method is described. The higher order source (HOS) is then defined and shown to subsume various cylindrical sound source types, including the vibrating cylinder and source-on-cylinder configurations. The proposed image-source method for directional sources is then formulated. Finally, several types of directional sources in rooms are simulated.

IMAGE-SOURCE METHOD

The reverberant sound field of the line source, the 2-D analogue to the acoustic monopole, can be simulated in a straight-forward manner in a rectangular room using the image-source method [8]. This method is based on geometric acoustics, where the reflection off a surface is modelled by the placing an image-

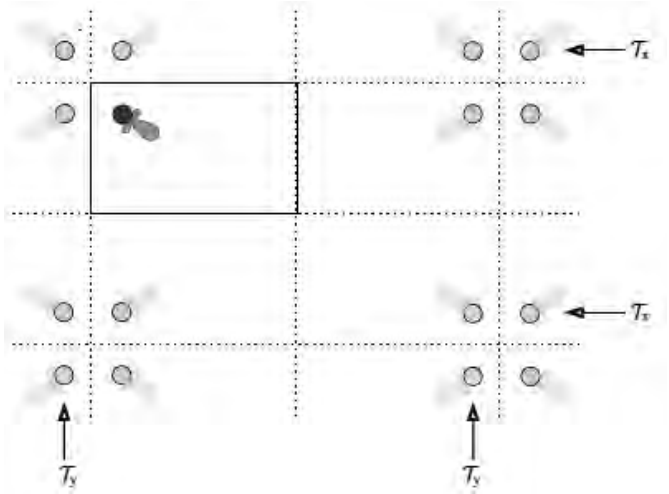

Figure 1. The lattice of image-sources in a rectangular room. Shown is the mirroring of the directivity pattern of each source about the x and y axes which are denoted by transformation T_x and T_y respectively.

source equidistant to the surface on the other side. A lattice of such image-sources is obtained by multiply reflecting the sound source about the walls of the room. The lattice for a rectangular room is depicted in Figure 1.

An expression for the sound field in the room can be written by superposition of image-source sound fields. Following a negative time convention, the sound field in the room created a sound source $\boldsymbol{\ell}$ at angular frequency ω is:

$$P_\ell(\boldsymbol{x};\omega)e^{-i\omega t} = \frac{i}{4}e^{-i\omega t}\sum_{n=1}^{N_{\text{img}}}\xi_n H_0(k\|\boldsymbol{x}-\boldsymbol{y}_{n\ell}\|),$$

where N_{img} is the number of image-source locations, $y_{n\ell}$ is the position of the n^{th} image-source of sound source l, ξ_n is the accumulated reflection coefficient resulting from multiple reflection off the walls corresponding to image-source n [8] and $H_m()$ is the m^{th} order Hankel function of the first kind.

The image-source method can be extended to account for the angular dependence of the reflection coefficient, though this is rarely done in practice. In this paper, the method is extended to simulate the sound field of a solid higher order source. The extension of the image-source method to directional sources is developed below.

SOUND FIELD AROUND A DIRECTIONAL SOURCE

The sound field around an arbitrary directional source $\boldsymbol{\ell}$ with respect to an origin at its centre is:

$$P_\ell(\boldsymbol{x}^{(\ell)},\omega) = \sum_{n=-\infty}^{\infty}\beta_n^{(\ell)}H_n(kr^{(\ell)})e^{in\phi^{(\ell)}}, \quad r^{(\ell)} > r_0, \tag{1}$$

where $\beta^{(\ell)}_n$ is a sound field coefficient, $x^{(\ell)} = (r^{(\ell)};\Phi^{(\ell)})$ is the position in relation to the centre of the source, $H_n()$ is the n^{th} order Hankel function of the first kind and r_0 is a radius bounding the source. The sound velocity of this directional source for a negative time convention is derived from the Euler equation:

$$\boldsymbol{V}_\ell(\boldsymbol{x}^{(\ell)},\omega) = \frac{1}{i\omega\rho}\nabla P_\ell(\boldsymbol{x}^{(\ell)},\omega),$$

where ρ is the density of air and c is the speed of sound in air. Substituting (1) into this expression and applying the gradient rule:

$$\nabla P = \frac{\partial P}{\partial r}\hat{\boldsymbol{e}}_r + \frac{1}{r}\frac{\partial P}{\partial \phi}\hat{\boldsymbol{e}}_\phi,$$

where $\mathbf{e}_r$ is the radial unit vector in the direction of x and $\mathbf{e}_\Phi$ is the tangent unit vector making an angle of $\Phi + \pi = 2$ with the horizontal axis, the velocity vector field at position $x^{(\ell)}$ can be written:

$$V_\ell(\boldsymbol{x}^{(\ell)},\omega) = \frac{1}{ic\rho}\sum_{n=-\infty}^{\infty}\beta_n^{(\ell)}\left[H_n'(kr^{(\ell)})\hat{\boldsymbol{e}}_{r^{(\ell)}} + \frac{in}{kr^{(\ell)}}H_n(kr^{(\ell)})\hat{\boldsymbol{e}}_{\phi^{(\ell)}}\right]e^{in\phi^{(\ell)}}.$$

The sound field shall be computed in a circular region of interest of radius r_c centred about the origin, due to cylindrical sources positioned external to the region of interest in a reverberant room.

The sound fields for several directional sources are summarized below including an arbitrary vibrating cylinder, a line source on a cylinder, an array of line sources on a cylinder.

Sound Field of a Higher Order Source

The sound created by a cylinder vibrating in an arbitrary fashion is now determined, with the goal of deriving the sound field of a source with an arbitrary directivity pattern.

Construct a general height invariant N_a^{th} order directional loudspeaker as a vertical vibrating cylinder of outward-going radial surface velocity $V_l(a,\Phi^{(\ell)})$ at each angle $\Phi^{(\ell)}$. Following [13], the radial velocity may be expressed by the Fourier representation:

$$V_\ell(a,\phi^{(\ell)}) = \sum_{n=-N_a}^{N_a} v_{n\ell} e^{in\phi^{(\ell)}} \qquad (2)$$

where $v_{n\ell}$ is the vibration coefficient of the n^{th} mode of source ℓ and N_a is the order of the sound source.

The radial surface velocity is directly proportional to the pressure gradient on the surface of the cylinder. Adopting a negative time convention, the relation is:

$$V_\ell(a,\phi^{(\ell)}) = \frac{1}{ikc\rho}\frac{\partial}{\partial r^{(\ell)}}\left[P(r^{(\ell)},\phi,\omega)\right]\Big|_{r^{(\ell)}=a}. \quad (3)$$

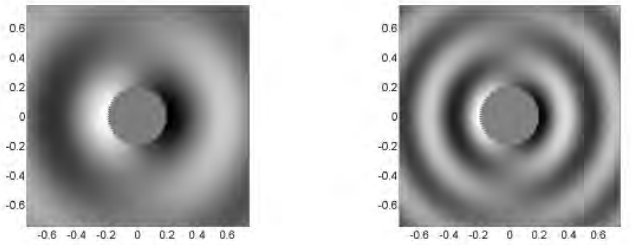

(a) 1st order, 500 Hz (b) 1st order, 1 kHz

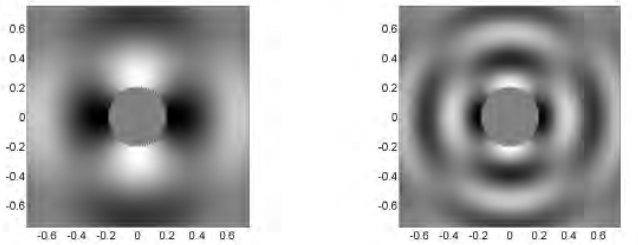

(c) 2nd order, 500 Hz (d) 2nd order, 1 kHz

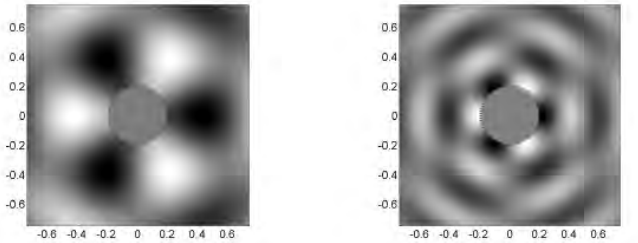

(e) 3rd order, 500 Hz (f) 3rd order, 1 kHz

Figure 2. Modes of vibration of a hard cylinder of radius 0.2m at 500 Hz and 1 kHz. The real part of sound pressure is shown.

Substituting Fourier expansion (2) and directional source expression (1) into (3), and equating each term of the series:

$$v_{n\ell} = \frac{1}{ic\rho}\beta_n^{(\ell)} H_n'(ka). \qquad (4)$$

The sound field around this arbitrary directional source is:

$$P_\ell(x^{(\ell)},\omega) = \sum_{n=-N_a}^{N_a} \underbrace{\frac{ic\rho}{H_n'(ka)} v_{n\ell}}_{\beta_n^{(\ell)}} H_n(kr^{(\ell)}) e^{in\phi^{(\ell)}}, \qquad (5)$$

where the sound field coefficient is underbraced. This equation expresses the sound field as that of a linear sum of higher order sources $H_n(kr^{(\ell)})e^{in\Phi^{(\ell)}}$ each with weighting $v_{n\ell}/H'_n(ka)$ up to the maximum order N. The sound fields of several vibrational modes for a cylinder of radius 0.2m are plotted in Figure 2.

The cylinder modes exhibit an activation property which is dependent on frequency [13]. In Figure 3 the strengths of the cylinder modes $H_n(kr^{(\ell)})/H'_n(ka)$ in the far-field are plotted for all modes active under 1 kHz. A vibrating cylinder of fixed radius has a low order directivity pattern at low frequencies and high order directivity pattern at high frequencies.

The modal response of real loudspeakers may vary. The sound field created by a point source, which is derived below, includes an additional factor of ℓ=k which creates a decay of 20 dB / decade in the modes at high frequencies. Loudspeakers such as electrodynamic loudspeakers include similar frequency dependent factors [1, p. 192].

By operating largely in their mass-controlled region, they produce a sound velocity which varies with the reciprocal of frequency. Due to the radiation impedance of air, this causes the decay at high frequencies.

In the far-field, the sound field can be derived from (5) using the asymptotic expansion of the Hankel function [14]:

$$P_\ell(x^{(\ell)},\omega) \to ic\rho\sqrt{\frac{2}{\pi r^{(\ell)}}} e^{i(kr^{(\ell)}-\pi/4)} \sum_{n=-N_a}^{N_a} \frac{i^{-n} v_{n\ell}}{H_n'(ka)} e^{in\phi^{(\ell)}}$$

The far-field directivity pattern of loudspeaker ℓ at angle Φ is then:

$$D_\ell(\phi) = \sum_{n=-N_a}^{N_a} i^{-n} \frac{v_{n\ell}}{H_n'(ka)} e^{in\phi}.$$

Loudspeaker directivity is a function of both the surface radial velocity controlled by the vibration modes and the cylinder radius which determines the number of active modes.

Sound Field of a Source on a Cylinder

The sound field due to a vertical line source at point $x^{(\ell)}$ about solid cylinder ℓ is [15, 16]:

$$P_\ell(x^{(\ell)},\omega) = \frac{i}{4}\sum_{n=-N}^{N}\left[J_n(kr_s) - \frac{J_n'(ka)}{H_n'(ka)}H_n(kr_s)\right] \times e^{-in\phi_s} H_n(kr^{(\ell)}) e^{in\phi^{(\ell)}}, \quad r^{(\ell)} > r_s$$

for the source positioned at r_s around a cylinder of radius a and $x^{(\ell)}$ is the position in relation to the centre of cylinder ℓ. Due to the high-pass nature of the Bessel functions in order n, the series is allowed to be truncated to $|n| < N = ekr_s/2$ [17].

To determine the sound field of a line source on the cylinder, set $r_s = a$ and apply the Wronskian relation:

$$J_n(x)H_n'(x) - J_n'(x)H_n(x) = \frac{2}{\pi i x},$$

applicable for the Hankel function of the first kind, to obtain:

$$P_\ell(\boldsymbol{x}^{(\ell)}, \omega) = \sum_{n=-N_a}^{N_a} \underbrace{\frac{P_0}{2\pi ka} \frac{e^{-in\phi_s}}{H_n'(ka)}}_{\beta_n^{(\ell)}} H_n(kr^{(\ell)}) e^{in\phi^{(\ell)}}, \tag{6}$$

where $N_a = \lfloor eka/2 \rfloor$. The sound field of a line source on a cylinder of radius 0:2m is again plotted in Figure 4.

Sound Field of a Circular Array on Cylinder

Now consider the sound field created by an array of line sources spaced around the surface of cylinder ℓ at polar angles $\{\Phi_1,...,\Phi_p\}$ with source excitation signals $G_{1\ell},...,G_{p\ell}$. The sound field for the circular array of P loudspeakers around solid cylinder ℓ is given by (1) where each sound field coefficient is:

Substituting (7) into (4), the vibrating cylinder mode coefficients

$$\beta_n^{(\ell)} = \frac{P_0}{2\pi ka H_n'(ka)} \sum_{p=1}^{P} G_{p\ell} e^{-in\phi_p}. \tag{7}$$

are:

$$v_{n\ell} = \frac{1}{ic\rho} \frac{P_0}{2\pi ka} \sum_{p=1}^{P} G_{p\ell} e^{-in\phi_p}.$$

A circular array of sources on a cylinder can hence be simulated

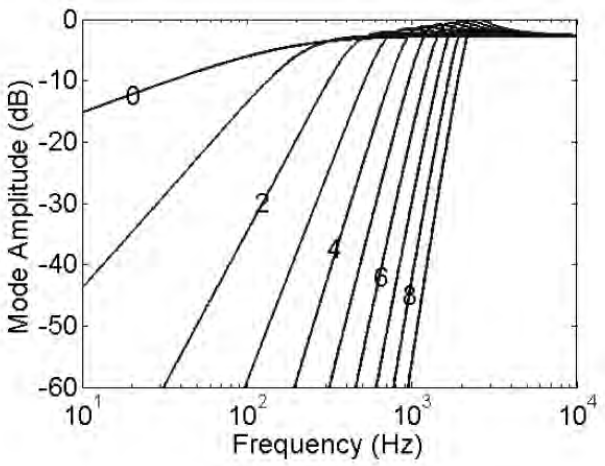

Figure 3. Amplitudes of the modes of vibration for n = 0,...,9 as a function of frequency of a hard cylinder of radius 0.2m.

with an equivalent vibrating cylinder modes $v_{n\ell}$, for $n = -N_a,...,N_a$.

The next section computes the sound field coefficients in a region of interest via a change of origin.

IMAGE METHOD FOR DIRECTIONAL SOURCES

The image-source method for directional sources requires both a translation of a source and a mirroring of a source directivity pattern about a wall. The translation or change of origin method shall be used to derive a computationally efficient method for determining the image-source method in the room. To complete the method, operations shall be defined to mirror the directivity pattern about the x and y axes.

Translation

The sound field in a circular region of interest of radius r centred about a global origin due to a directional source positioned outside the region of interest shall now be determined.

Let the cylinder be at position y_ℓ in a global coordinate system,

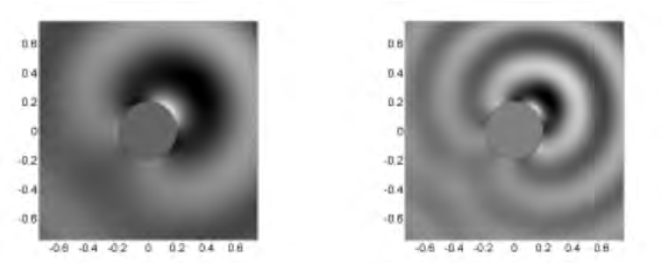

(a) 500 Hz (b) 1 kHz

Figure 4. Line source on a hard cylinder of radius 0.2m positioned at polar angle 45° at 500 Hz and 1 kHz. The real part of sound pressure is shown.

whose origin $\mathcal{O}$ is centred at the region of interest. The sound field around the cylinder is expressed in terms of vector $\mathbf{x}^{(\ell)}$ in reference to origin $\mathcal{O}_\ell$ at the centre of cylinder ℓ. As shown in Figure 5, a change of origin to the global coordinate system is made by writing $\mathbf{x}^{(\ell)} = \mathbf{x}\text{-}\mathbf{y}_\ell$. Using the Bessel function addition formula [18, p. 361], the sound field can be expanded around the global origin:

for $r < R_\ell$ where the series truncation $N_r = ekr_c/2$ is accurate for

$$H_m(kr^{(\ell)})e^{im\phi^{(\ell)}} = \sum_{n=-N_r}^{N_r} H_{n-m}(kR_\ell)e^{-i(n-m)\theta_\ell} \times J_n(kr)e^{in\phi},$$

a region of interest of radius r_c.

Substituting this into (1), the pressure in the region of interest due to directional sound source ℓ is written:

$$P_\ell(\boldsymbol{x},\omega) = \sum_{n=-N_r}^{N_r}\left[\sum_{m=-N_a}^{N_a}\beta_m^{(\ell)}H_{n-m}(kR_\ell) \times e^{-i(n-m)\theta_\ell}\right]J_n(kr)e^{in\phi} \quad (8)$$

for $r < R_\ell a$ or:

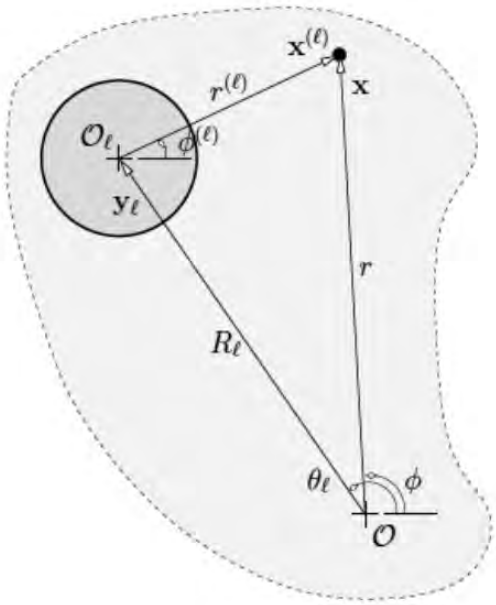

Figure 5: The change of origin for expressing sound pressure around a cylinder with origin $\mathcal{O}_\ell$ in terms of a global coordinate system with origin $\mathcal{O}$.

where $\beta_{n\ell}$ represents the sound field coefficient in the region of interest for loudspeaker ℓ:

$$P_\ell(\boldsymbol{x},\omega) = \sum_{n=-N_r}^{N_r} \beta_{n\ell} J_n(kr) e^{in\phi}, \qquad (9)$$

This equation is a linear convolution of the modes $H_n(kR_\ell)\, e^{-in\Theta l}$ with the sound field coefficients $\beta_n^{(\ell)}$ about the sound source origin $\mathcal{O}_\ell$[2]. A change of origin in 2-D is in essence accomplished by a linear convolution. This is much simpler than in 3-D where translation of basis functions requires the calculation of Clebsh-Gordan coefficients [19, p. 93-122]. The sound velocity vector field in the region of interest for the sound pressure field in (9) is:

$$\beta_{n\ell} = \sum_{m=-N_a}^{N_a} \beta_m^{(\ell)} H_{n-m}(kR_\ell) e^{-i(n-m)\theta_\ell}. \qquad (10)$$

By comparison, the sound field due to a line source located at y in free-space can be expressed [14]:

$$\boldsymbol{V}_\ell(\boldsymbol{x},\omega) = \frac{1}{ic\rho} \sum_{n=-N_r}^{N_r} \beta_{n\ell} \left[J_n'(kr)\hat{\boldsymbol{e}}_r + \frac{in}{kr} J_n(kr)\hat{\boldsymbol{e}}_\phi \right] e^{in\phi}.$$

The sound field coefficient $\beta_{n\ell} = i/4H_n(kR_\ell)e^{-in\Theta l}$ can equivalently be obtained from (10) by setting β_m^ℓ to that corresponding to a line source located at $\mathcal{O}_\ell$, i.e.:

$$\frac{i}{4} H_0(k\|\boldsymbol{x}-\boldsymbol{y}_\ell\|) = \frac{i}{4} \sum_{n=-N_r}^{N_r} H_n(kR_\ell) e^{-in\theta_\ell} J_n(kr) e^{in\phi}$$

which helps to validate (10).

$$\beta_m^\ell = \begin{cases} \frac{i}{4}, & m = 0, \\ 0, & m \neq 0. \end{cases}$$

Mirroring

When generating the image-sources for a directional source, the sound field of the directional source must be reflected in addition to the source being translated. This mirroring of image-source directivity patterns are depicted in Figure 1 for the rectangular room.

Assume the axes align with the perpendicular walls of the room. This sound field must then be mirrored about the x and y axes. The reflection of the coefficients $\beta_n^{(\ell)}$ through any combinations of axes shall be represented with a set of transform operators T . The simplest transform to consider is the identity transform, for which $T_1\{\beta_n^{(\ell)}\} = \beta_n^{(\ell)}$. Single axes reflections shall be represented using the operators T_x and T_y.

The transforms used to perform these reflection operations is summarised in Table 1. By way of example, the reflection of the 2-D basis function $H_n(kr^{(\ell)})e^{in\Phi^{(\ell)}}$ about the x axis where $\Phi^{(\ell)}$ tends to $-\Phi^{(\ell)}$ is given by:

$$(-1)^n H_{-n}(kr^{(\ell)}) e^{-n\phi^{(\ell)}}.$$

This result is used to write the transformations that occur on the sound field coefficients:

$$\mathcal{T}_x\{\beta_n^{(\ell)}\} = (-1)^n \beta_{-n}^{(\ell)}.$$

The reflection operators are both commutative: $T_x \circ T_y = T_y \circ T_x$ and self-inverses: $T_x \circ T_x = T_y \circ T_y = T_I$. Because T_x and T_y are self-inverses, mirroring about the x or y axis an even number of times results in an identity operation.

In Figure 1, these properties are shown. The image-sources resulting from reflection off the horizontal (vertical) walls an odd number of times are marked with arrows. The intersection of horizontal and vertically pointing arrows are where image-sources are reflected about both x and y axes ($T_x \circ T_y$). All other image-sources remain unchanged by the wall reflection (T_I). Each image-source hence possesses one of four different sets of sound field coefficients, each derived from the original source coefficients $\beta_n^{(\ell)}$.

Proposed Methods for Directional Sources

The sound field in the room is obtained by summing the sound field contribution from each image-source. The sound pressure at a point in the region of interest due to L cylindrical directional sources at $y_0^{(\ell)} = (R_\ell;\Theta_\ell)$ are determined using one of two methods proposed below.

These methods presume that the lattice of image-source locations $\{y_{n\ell}\}_n$ and corresponding accumulated reflection coefficients $\{\xi_n\}_n$ in the rectangular room for each source ℓ have been pre-computed using the methods in [8]. For simulations, all the images lying within a distance cT_{60} corresponding to propagation distance of one reverberation time from the centre of the room are typically included in the computation. The methods for determining the sound field over the room are:

Algorithm A Without using the change of origin formula, the sound field can be determined directly using an image-source method. For each point of interest **x**, the vector from the origin of each imagesource n of loudspeaker l, $\mathbf{x}^{(\ell,n)}$ $\mathbf{x}$-$\mathbf{y}_{n\ell}$, must be calculated. We write vector $\mathbf{x}^{(\ell,n)}$ in the polar form $(r^{(\ell,n)}, \Phi^{(\ell,n)})$. The sound field must be computed from each image-source at each point in the room using (5):

$$P_\ell(\boldsymbol{x},\omega) = \sum_{n=0}^{N_{\text{img}}} \zeta_n \sum_{m=-N}^{N} \beta_m^{(\ell,n)} H_m(kr^{(\ell,n)}) e^{in\phi^{(\ell,n)}}, \qquad (11)$$

where $\beta_m^{(\ell,n)} = T_n\{\beta_m^{(\ell)}\}$, $T_n\{\}$ is the correct mirroring operator to apply to image-source n and $\beta_m^{(\ell)}$ is obtained from $v_{m\ell}$ using (4).

Algorithm B Using the change of origin formula, the calculation is broken into two steps. In step one, the coefficients of the

Table 1: Transforms to reflect a sound field about the x and/or y axes for loudspeaker l.

Operator	Angle Transform	Coefficient
$\mathcal{T}_x$	$\phi^{(\ell)} \to -\phi^{(\ell)}$	$(-1)^n \beta_{-n}^{(\ell)}$
$\mathcal{T}_y$	$\phi^{(\ell)} \to \pi - \phi^{(\ell)}$	$\beta_{-n}^{(\ell)}$
$\mathcal{T}_x \circ \mathcal{T}_y$	$\phi^{(\ell)} \to \pi + \phi^{(\ell)}$	$(-1)^n \beta_n^{(\ell)}$

sound field in the room are computed:

$$\beta_{m\ell} = \sum_{n=0}^{N_{\text{img}}} \zeta_n \left[H_m(kR_n^{(\ell)}) e^{-im\theta_{n\ell}} * \mathcal{F}_n\{\beta_m^{(\ell)}\} \right], \quad (12)$$

where * is the convolution operator corresponding to change of origin formula (10) and $(R_{n\ell}, \Theta_{n\ell})$ $y_{n\ell}$ is the n^{th} images location of the cylindrical source l. In step two, these coefficients are used to compute the sound field using the interior expansion [14]:

$$P_\ell(\boldsymbol{x}, \omega) = \sum_{m=-N_r}^{N_r} \beta_m J_m(kr) e^{im\phi}. \quad (13)$$

This two-step algorithm is also the basis of the fast multipole method (FMM). It has been used for speeding the computation of the image-source method for monopole sources [11]. It is extended here to the case of directional sound sources.

These algorithms are applicable to calculating the sound field in a region which does not enclose any sound sources. To compute the field over a room, algorithm B must be modified slightly. since (12) only applies for interior regions where there are no sources. As shown in Figure 6, some sources lie closer to the origin than some positions of interest in the room. Equation (12) is not applicable for such sources. Assume the global origin O is in the centre of the room. Define D as the distance from O to the farthest corner of the room. For successful calculation in Algorithm B, the sound source and the one or two image-sources which lie within distance D from the centre of O must be excluded from the calculation in (12). Their contribution to the sound field can be computed separately using (11).

Algorithm B retains significant computational benefit over Algorithm A. The exclusion of some image-sources from the fast approach of Algorithm B does not subtract from its computational speed, because the number of such sound sources is so few. The computational complexity of using proposed methods is presented in the next section.

Computational Aspects

Several computational aspects of the proposed algorithms will now be discussed. Visualisation of a sound field requires sampling over a dense grid. The numbers of imagesources required for accurate simulation, depending upon the wall absorption coefficient, may also be large. Below, the numbers of grid points and image-sources required for the simulation methods are determined. The computational complexities of the two algorithms shall then be compared. A rule for whether to choose the direct Algorithm A or the two step Algorithm B is then devised.

Spatial Sampling Requirements

Consider computing the sound pressure P(x,w) over a room. Sound pressure shall be spatially sampled over a lattice of M points $x_1,...,x_M$ up to a maximum frequency f. A minimum number of lattice points is required for accurate visualization of the sound field. The largest number of spatial samples are required for frequency f for which the wavelength is $\lambda = c / f$. In a room of dimensions L_x x L_y, for visualization of a traveling wave it is reasonable to sample the field with 8 or more points per wavelength (see Figure 7). This implies sampling a N_x x N_y grid of sample points, where $N_x = [8L_x/\lambda]$ and $N_y = [8L_y/\lambda]$. The total number of pressure samples $N_p = N_x N_y$ is hence proportional to f^2.

Image-Source Numbers

There is approximately one image-source for every area of the room $A = L_x L_y$. For the T_{60} reverberation time, there are hence approximately $\pi(cT_{60})^2/A$ total imagesources for each sound source $\boldsymbol{\ell}$. Ignoring air absorption, T_{60} can be estimated from the wall reflection coefficient using the Sabine reverberation time [20]:

$$T_{60} = \frac{\ln 10^6}{c\bar{\alpha}} \lambda_{\text{mfp}},$$

where λ_{mfp} is the mean free path in a 2-D room given by $\lambda_{mfp} = \pi A/P$ and $P = 2(L_x+L_y)$ is the length of the room perimeter. The number of image-sources can hence be estimated as:

$$N_{\text{img}} \approx 5.92 \times 10^3 \frac{\mathscr{A}}{\mathscr{P}^2 \bar{\alpha}^2},$$

where α is the average wall absorption coefficient.

Using statistical room acoustics [20], several other useful room acoustic quantities can be obtained which are summarized in Table 2.

Table 2. Statistical room acoustic quantities for a 2-D room of area A , length of room perimeter P and average wall absorption coefficient α. Π is the radiating power of the sound source, DI is the source directivity index in the direction of interest and r is the distance from the source.

Quantity	Symbol	Equation
Reverberation time	T_{60}	$\frac{6\ln 10\pi}{c\bar{\alpha}} \frac{\mathscr{A}}{\mathscr{P}}$
Reverberant energy density	ε_r	$\frac{\pi}{c\mathscr{P}\bar{\alpha}}\Pi$
Direct energy density	ε_d	$\frac{\mathrm{DI}}{2\pi rc}\Pi$

The direct and reverberant energy densities for a sound source with radiating power P are shown. From these, the critical distance at which the direct and reverberant components are of equal energy density is:

$$r_{cr} = \frac{\mathscr{P}\bar{\alpha}\mathrm{DI}}{2\pi^2},$$

where DI is the directivity index in the source direction of interest.

Computational Complexity

The heaviest computational task involved in the imagesource method is calculating basis functions. The mode functions $H_n(kR)e^{in\Theta}$ and $J_m(kr)e^{im\Phi}$ must typically be computed over a large number of positions. An analysis of computational complexity can be based on the number of basis functions to be computed.

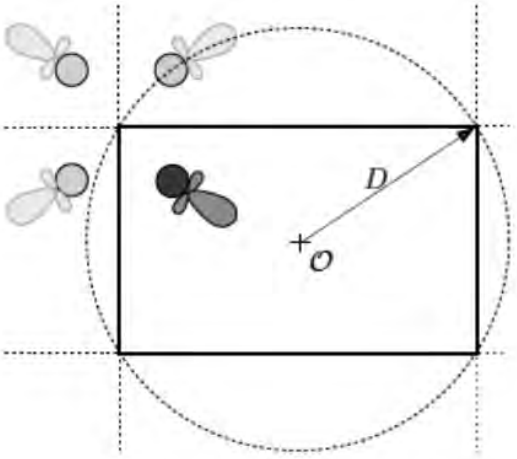

Figure 6. Shown are the direct source and an image-source lying within a circle circumscribing the room.

Algorithm A For each image-source, the sound field is computed over N_p points using the mode expansion of $2N_a+1$ terms in (5). This constitutes computed each the set of basis functions $H_m(kr^{(\ell,n)})\, e^{im\phi^{(\ell,n)}}$; $m = -N_a,\ldots,N_a$ over each of the points for a total of $N_{img}N_p(2N_a+1)$ basis function calculations for each source.

Algorithm B The modal coefficients of the sound field are first calculated in the room by determining $H_m(kR_\ell)e^{-im\Theta\ell}$ for the active modes of each imagesource. For a room of circumscribed radius D, $2N_r+1 = 2e\pi D/\lambda +1$ modes are active. For all image-sources, this totals $N_{img}(2N_r+2N_a+1)$ terms to perform the convolution. The sound field is then computed at each of N_p points by summing over the modes, requiring calculation of $(2N_r+1)N_p$ terms of $J_m(kr)e^{im\phi}$. The total is $(N_{img}+N_p)(2N_r+1)+2N_{img}N_a$ mode computations for each source.

The parameters N_a and N_r are usually dependent on frequency. At higher frequencies, the room supports more modes and a sound source has more modes of vibration.

Whilst the computation in Algorithm A is related to the product of N_{img} and N_p, for Algorithm B it is related to their sum, which may be much smaller. That is, the complexity of Algorithm A is $O(N_{img}\, f^3)$ while that of Algorithm B is $O(f^3)+O(N_{img}f)$.

The decision to choose Algorithm B over Algorithm A is based on the relative sizes of N_p and N_r. Based on the above reasoning, the decision rule is:

$$N_p \underset{A}{\overset{B}{\gtrless}} \frac{(2N_a+2N_r+1)N_{\text{img}}}{(2N_a+1)N_{\text{img}}-(2N_r+1)}. \qquad (14)$$

Because the total number of modes of the image-sources $N_{img}(2N_a+1)$ is usually much greater than the numbers of modes active in the room $2N_r+1$, Algorithm B is expected to be much more efficient for room simulation.

Computing the sound field for a higher order source is more time consuming than it is for an omnidirectional source. In fact, it becomes $2N_a+1$ times more timeconsuming, without the FMM-based method Algorithm B. It becomes more critical to use a multipole method for the case of directional sound sources.

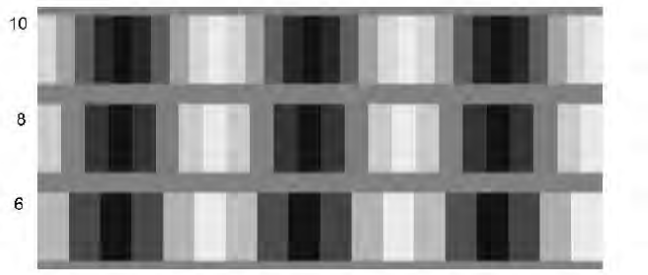

Figure 7. Plot of sine wave with 6, 8 and 10 pixels per period.

SIMULATION EXAMPLE

A single directional source shall now be simulated in a 6.4 x 5m room. Figure 8 shows the sound field at 750 Hz in the room for an acoustic monopole, a dipole and a third order pencil beam. The wall absorption coefficient here was set to 0.25 so that the influence of the source directivity pattern is clearly seen. The critical distance is 1.18 cm for a monopole, 2.36m for a dipole in the direction of the two lobes and 8.2 m for a third order beampattern in its main lobe direction. In Figure 8(a) and 8(b) the direct field dominates over the reverberant field up to the critical distance, whilst in Figure 8(c) the direct field is shown to dominate up to the room boundary.

With regard to computations aspects, to simulate in the room up to 1 kHz, at least a 150 x 120 grid of points would be recommended from above. For calculating sound pressure over this grid, the number of active modes in the room $2N_r+1$ at a frequency of 1 kHz is 204. For third order source in a room with α = 0.51, $1.77\text{x}10^8$ mode functions must be computed under Algorithm A and $7.94 \text{ x } 10^6$ mode functions must be computed under Algorithm B. To simulate omnidirectional sources in this example it is significantly more worthwhile to choose Algorithm B over Algorithm A. Applying (14), Algorithm B would still be worthwhile when the number of locations is $N_p > 239$. For directional sources, it is of even more benefit to use Algorithm B. For third order sources for example, it is worthwhile to use Algorithm B for only 31 locations.

The 2-D image-source simulator is more efficient to implement than a 3-D simulator. In 2-D, the numbers of image-sources is proportional to $(T_{60})^2$ whilst in 3-D, they are proportional to $(T_{60})^3$. In the example 2-D room, the reverberation time is 350 msec with 1400 image sources and an α of 0.51. In a 3-D room of dimensions 6.4 x 5 x 4m with the same α , the reverberation time is only 250 msec yet 28,000 image-sources are required which is an order of magnitude more.

FURTHER DISCUSSION

The 2-D method of sound field simulation is well-suited to the simulation of surround sound systems. A 2-D method is useful in particular for simulating 2.5-D surround sound systems, where both the loudspeaker and the listeners lie within the same horizontal plane [21]. Though these systems are unable to create out-of-plane sound effects, more practical numbers of loudspeaker drivers are required to control the sound field than for the 3-D case. The simulator helps establish the expected performance of surround systems in rooms.

However, due care must be taken in applying this simulation to real-world situations. By the stationary phase approximation, the 2-D model is strictly accurate in the x-y plane for sufficiently tall higher order sources. For real sources the approximation breaks down in the farfield. A key difference between 2-D and 3-D is that in 3-D the amplitude of sound pressure decays in proportion to the inverse of radius whilst in 2-D it decays according to the square root of radius [22].

The image-source method is exact for the case of a line source with perfectly rigid walls. It lends most of its application to modeling the wall absorptive cases, which it does approximately. The exact solution in this case requires a solution of the wave equation that results in complex wall reflection coefficients [20]. There are many physical other phenomena that occur in a real room not accounted for by image-source methods, including local temperature and humidity fluctuations. Yet due to its convenience, the image-source method is still commonly in use.

The image-source method is a specular reflection model. It does not account for diffuse reflections which are caused by rough surfaces. For a diffuse reflection, the angle of incidence no longer equals the angle of reflection. Instead, the sound is scattered in all directions as described by Lambert's cosine law [20, p. 81]. In [23], the image-source method was extended for diffuse reflection by replacing each image-source with a continuum of image-sources arranged on a line. In this manner, reflections are made to approximately preserve Lambert's cosine law. In future work, we shall investigate extending this approach to directional sources.

The proposed method does not model multiple scattering between cylinders. Multiple reflection of sound between closely-spaced cylinders cause interactions that cannot be modelled by a simple image-source approach. The method is thence inaccurate unless cylindrical sources are located at several cylinder radii away from walls or other cylinders for these interactions to be negligible [24]. This is not an unreasonable assumption. In the simulation of surround systems for example, it is safe to assume that loudspeakers are spaced apart. Doing so allows the system to better create spatial sound.

An alternate method to simulating the directional sources is to replace each solid source with an equivalent array of simple sources in free-space. Each cylinder could for example be replaced with a circular array of radius a of $2N_a+1$ line sources. The strength of this simulation method is that the original image-source method, which is efficiently implemented in a FMM manner [11], can be used directly. However this scheme introduces problems with inaccuracy. Circular arrays of simple sources cannot create certain sound fields. In particular, they cannot support creation of the sound field at frequencies for which the Bessel functions of ka are zero [15]. Furthermore, because of the added computation of emulating a directional source with simple sources, the method offers no computational benefit.

CONCLUSION

This paper extends the image-source method to computing the field for a set of sound sources with arbitrary directional patterns. Here the sound field is efficiently calculated over an extended area using a fast multipole method. The image-source method is applicable for multiple numbers of directional sources, provided sources are spaced several source dimensions away from other obstacles so that multiple scattering can be neglected.

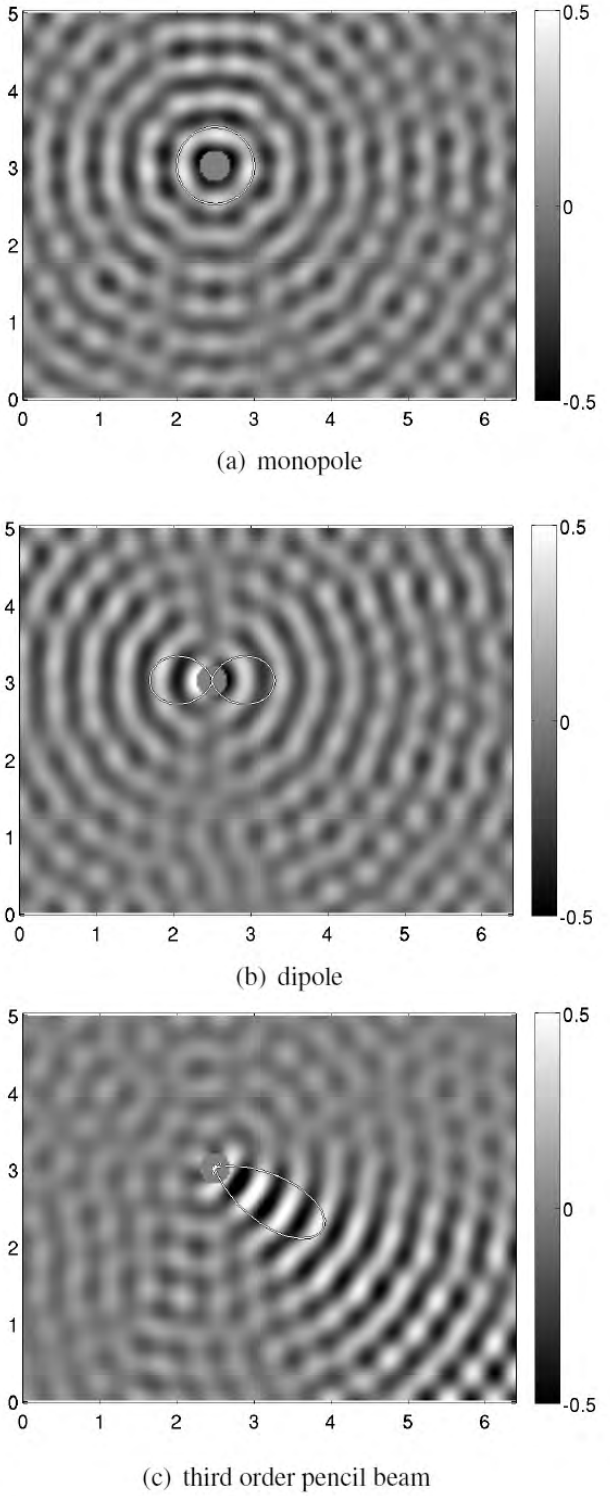

Figure 8. Sound field of a vibrating cylinder of radius a = 0.2 at 750 Hz for a (a) monopole, (b) dipole and (c) third order pencil beam in a room generated by the proposed image-source method with a 0.25 wall absorption coefficient. Far-field directivity patterns are shown.

ACKNOWLEDGEMENTS

This paper was written using funds from the New Zealand Ministry for Science and Innovation.

REFERENCES

[1] L.L. Beranek, Acoustics, Acoustical Society of America, New York, 1993.

[2] T. Holman, "Dipolar confusion: The case for dipole loudspeakers," Stereo review, 1998.

[3] K. Kowalczyk and M. Walstijn, "Wideband and isotropic room acoustics simulation using 2-D interpolated FDTD schemes," IEEE Trans. Speech and Audio Processing, vol. 18, no. 1, pp. 78–89, 2010.

[4] M. Kleiner, B. Dalenback, and P. Svensson, "Auralization -an overview," Journal of the Audio Engineering Society, vol. 41, no. 11, pp. 861–875, 1993.

[5] A. Pietrzyk, "Computer modeling of the sound field in small rooms," in Proc. of the 15th AES Int. Conf. on Audio, Acoustics and Small Spaces, 1998, vol. 2, pp. 24–31.

[6] Y. Kahana and Philip A. Nelson, "Numerical modelling of the spatial acoustic response of the human pinna," Journal of Sound and Vibration, vol. 292, no. 1, pp. 148–178, 2006.

[7] M.E. Johnson, S.J. Elliott, and K.H. Baek, "An equivalent source technique for calculating the sound field inside an enclosure containing scattering objects," J. Acoust. Soc. Am., vol. 104, no. 1, pp. 1221–1231, 1998.

[8] J. Allen and D. Berkley, "Image method for efficiently simulating small-room acoustics," Journal of the Acoustical Society of America, vol. 65, no. 4, pp. 943–950, 1979.

[9] P. Peterson, "Simulating the response of multiple microphones to a single acoustic source in a reverberant room," Journal of the Acoustical Society of America, vol. 80, no. 5, pp. 1527–1529, 1986.

[10] Eric A. Lehmann and Anders M. Johansson, "Image method for efficiently simulating small-room acoustics," Journal of the Acoustical Society of America, vol. 124, no. 269, pp. 269–278, 2008.

[11] R. Duraiswami, D. N. Zotkin, and N. A. Gumerov, "Fast evaluation of the room transfer function using multipole expansion," IEEE Transactions on Speech and Audio Processing, vol. 15, pp. 565–576, 2007.

[12] A. Wabnitz, C Jin, N. Epain, and A. Schaik, "Room acoustic simulation for multichannel microphone arrays," in Proceedings of the International Symposium on Room Acoustics (ISRA), 2010.

[13] M.A. Poletti, T.D. Abhayapala, and P. Samarasinghe, "Interior and exterior sound field control using general two dimensional higher-order variable-directivity sources," J. Acoust. Soc. Amer., vol. 129, no. 5, pp. 3814–3823, 2012. ¶

Improving Acoustic Insulation Using Vibration-Damping Infills in Floors

Grant W. Emms

New Zealand Forest Research Institute, Private Bag 3020, Rotorua 3046, New Zealand

This paper was previously presented at the 21st Biennial ASNZ Conference, Wellington, NZ

Abstract

Historically timber-framed floor system designs have sometimes included some sort of granular material infill in order to reduce sound transmission between tenancies. Often this material is readily available and low cost material (e.g. ash, scoria, and sand). Recent research has been conducted into timber-framed floor toppings which contain a granular material infill in the form of a sand and sawdust mixture. The sand and sawdust infill increases the mass of the floor, which improves the low frequency impact insulation performance. This sand and sawdust infill also greatly increases the vibration damping in the upper part of the floor, improving the mid to high frequency sound insulation performance, while also making the system robust to construction defects. This paper presents results of isolated element impact insulation and flanking transmission measurements of timber-framed floors which have a sand and sawdust infill in the floor topping.

INTRODUCTION

This paper is an analysis of some recent measurements conducted on timber-framed floor toppings (Emms et al., 2006; Emms & Walther, 2010). The focus of this paper is the use of granular materials in floor topping system. The form of the granular materials considered is sand and sawdust mixtures. The granular material infill increases the mass of the floor, which improves the low frequency impact insulation performance. The granular material infill also greatly increases the vibration damping in the upper part of the floor, improving the mid to high frequency sound insulation performance, while also making the system robust to construction defects.

GRANULAR MATERIALS IN FLOORS

Granular or particle-type materials have been used quite frequently in the past as an infill in timber structures. It was not uncommon to have sand or fly ash in timber floors in parts of the United Kingdom many years ago – the fill would be either placed on shelves between the joists or on the ceiling (which was made of material which could support the weight). The primary function of this fill was for sound insulation purposes. Another example of this is found in some old multi-storey timber buildings in New Zealand (e.g.. the old parliament buildings in Wellington), where volcanic scoria was used in the floors. More modern references to this are found in Switzerland, where sand has been used as a layer in both retrofit and new buildings (Lappert & Geinoz, 1998). Incidentally, Lappert and Geinoz do note that the sand should be heated to ensure no living things are introduced.

Walk and Keller (2001) did recent work to develop a floor using a massive amount of 'granular' material on which a walking surface was floating. They do not say what exactly this granular

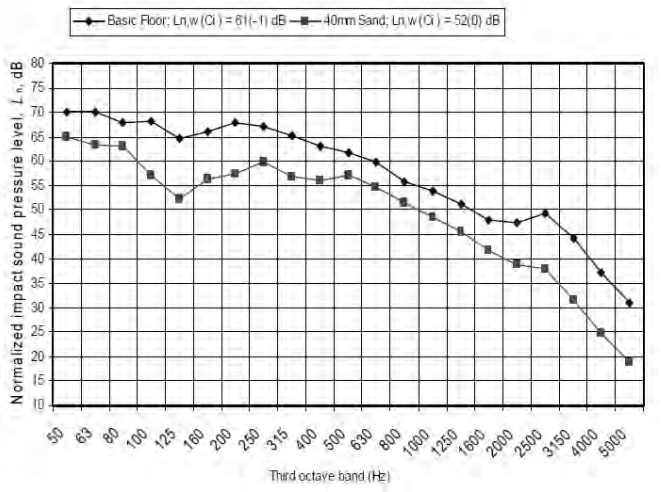

Figure 1. Comparison of the impact insulation performance of the 'Basic Floor' and '40mm Sand Floor'. Both floors are 3.2m by 7m (joist length).

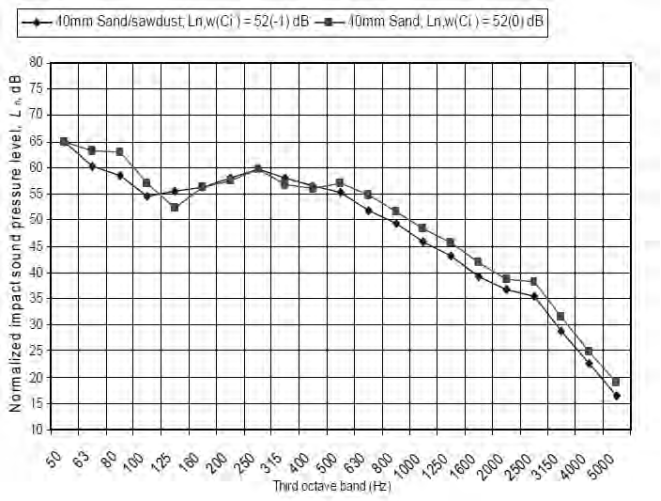

Figure 2. Comparison of the impact insulation performance of the '40mm Sand/Sawdust Floor' and '40mm Sand Floor'. Both are 3.2m by 7m.

Continued on Page 25...

Sylomer®

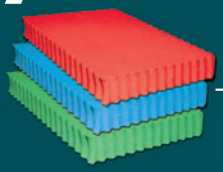

sold by Pyrotek noise control

made in **Germany**

renown **globally**

Getzner's Sylomer® and Sylodyn® are the leading materials on the international market for vibration technology.

They are elastic polyurethane materials (PUR elastomers), which deform when subjected to tension or compression loads, but always return to their original shape. In doing so, this materials isolate and reduce vibrations which can have negative effects on humans, the environment and materials.

Sylomer® and Sylodyn® have a wide stiffness range, allowing them to be used in a large range of applications in civil engineering and machinery. In most of them, they are used as elastic inter layers like a spring. The characteristics of this spring can be adapted to the need of application.

Pyrotek's sales engineers can support you with technical and design advice.

www.pyroteknc.com
exclusive agents
0800 226 878 427
(0800 ACOUSTICS)

...Continued from Page 23

Figure 3. View of plywood flooring over 70x45mm battens laid on the flat with sand infill.

material was and further communication with the authors did not reveal it, although they did say that it was being installed in a block of apartments. However, they said that the main reason for using this granular material was to take advantage of the high damping afforded by the granular material due to the friction between particles, because a lightweight floor, in their opinion, could never have enough mass to provide excellent sound insulation.

Granular material vibration damping

Since granular materials, particularly sand, have been used with some success in buildings as a way of improving vibration damping, it is worth overviewing some of the literature which exists about this.

A good account of the use of sand with other mixtures of materials has been provided by Kuhl and Kaiser (1962) for use with concrete structures. They tested various sands and mixtures (fine sand, course sand, brick rubble, and mixtures of sand and sawdust), and found that hard granular materials with sharp edges or with a soft material (e.g. sawdust or rubber dust) gave better damping at lower frequencies.

They thought that this was due to the sharp edges giving more friction with vibrational strains and the lower wavespeed of vibrations in the sand sawdust or rubber dust mixtures. The sand/sawdust mixture tested was 80/20 sand/sawdust. They also note that the impedance of the granular fill should try to match the impedance of the surrounding, structural material to enable maximum coupling of energy into the granular fill. They determined that the maximum damping was attained at cavity resonances in the granular fill. The damping was also found to be nonlinear in the sense that it depended on amplitude of the vibrations; higher amplitudes result in more movement of the granules and hence more friction.

Richards and Lenzi (1984) did measurements on the vibration damping due to sand and found that below a strain of 106 the particle movement is small and the damping in the sand is small and is probably not due to the friction of the particles; above that point damping becomes increasingly significant. They also noted that loose sand in cavities is useful because there is the added damping benefit of having the granules move around from regions of high density to regions of lower density. This movement is a maximum in resonances in the cavities which contain the granular fill.

Xu et al. (2005) noted that shear friction is the major contributing factor to the damping due to granular infills . Since our concern in low-frequency floor vibrations is the bending waves in the floor which would cause a lot of shearing of any infill, this is an important point to note.

Sun et al. (1986) observed from experiment that, when looking at sand laid on a vibrating metal plate, the vibrational damping in the plate is a maximum at frequencies above when the thickness of the sand is about equal to 0.05c, where λ_c is the longitudinal wavelength of the vibrations in the sand ($\lambda_c = c/f$, where c is the propagation speed of the vibrations (100 to 200 m/s for sand) and f is the frequency).

Below this point there is a sharp drop in damping, and above

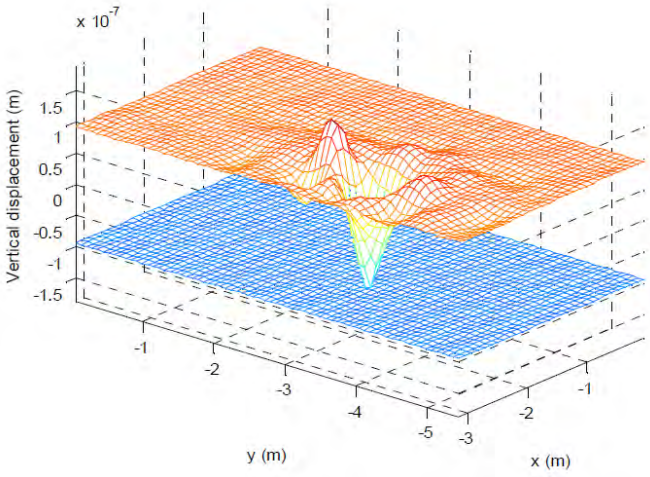

Figure 4. Measured vibration (displacment) of a Sand/ Sawdust floor upper surface and ceiling from 1N of forced vibration on the upper surface.

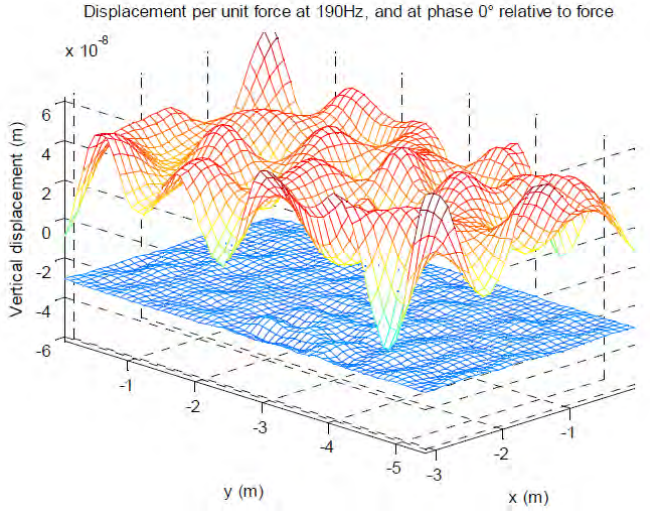

Figure 5. Measured vibration (displacment) of a Floating Gypsum Concrete floor upper surface and ceiling from 1N of forced vibration on the upper surface.

this point there is a gradual decrease (due to the increasing weight of the sand packing down the sand below and stopping movement of the sand granules).

Interestingly, sawdust is often mixed with sand when used for anechoic terminations for experiments with vibrations in beams. The sawdust is included to keep the sand from packing down, thereby improving its absorption characteristics.

IMPACT INSULATION MEASUREMENTS ON FLOORS WITH GRANULAR MATERIAL INFILLS

In this section we describe measurements that were done on a number of floor system elements which have a granular infill in the floor topping. The granular infill used was either paving sand, or a mixture of paving sand and sawdust.

The floor elements were tested in the same facility, with suppressed flanking sound transmission, and in accordance with standard ISO 140-6.

The following floors were tested:

- Basic Floor (Figure 12): A timber floor with plywood upper, solid timber floor joists, a fire-rated ceiling disconnected from the joists using rubber isolation clips, and filled with dense fibreglass.
- 40mm Sand Floor (Figure 13): The Basic Floor as a subfloor with a floor topping consisting of 40mm deep layer of sand between 45mm wooden battens, and another layer of plywood on the battens. The sand density is 1250 kg/m^3.
- 40mm Sand/Sawdust Floor (Figure 14): The Basic Floor with a floor topping consisting of 40mm deep layer of sand and sawdust between 45mm wooden battens, and another layer of plywood on the battens. The sand-sawdust mix is 60% sand and 40% sawdust by loose volume (density 1170 kg/m^3).

Measurement Results

In Figure 1 we can compare the results of the Basic Floor and the 40mm Sand Floor. The greater mass and damping of the floor upper has resulted in significant improvements to the impact insulation performance.

It was noted before that the addition of sawdust with sand does tend to improve the damping characteristics of sand alone. In Figure 2 we can compare the results of the 40mm Sand Floor and the 40mm Sand/Sawdust Floor. We note that although the mass has been slightly reduced by displacing sand with sawdust, the extra damping has resulted in an improvement of performance, particularly at the higher frequencies.

It should be noted that the floor uppers with the granular infill are not floating on the subfloor in any way. The separation of the additional layer of plywood is achieved through battens which are directly fixed to the subfloor surface (Figure 3). And the top layer of plywood is directly fixed to the battens.

There is no resilient isolation between layers. All the isolation is achieved through vibration absorption in the granular material. It is an inherently robust system.

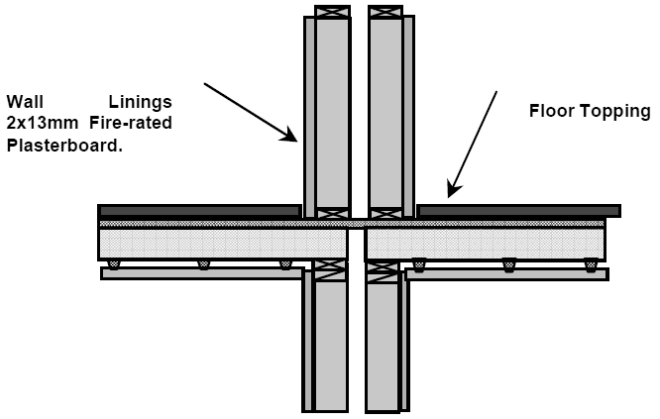

Figure 6. The form of the specimen tested for flanking transmission.

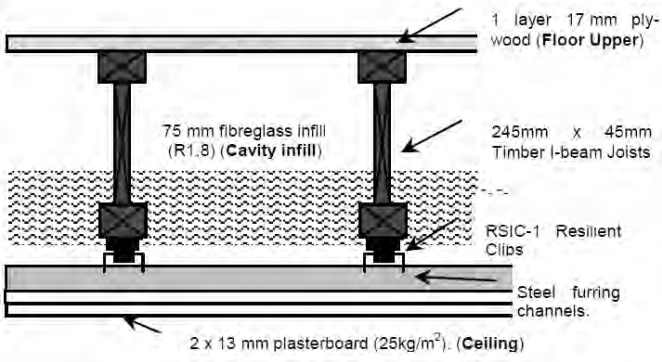

Figure 7. The basic subfloor used for the flanking transmission measurements.

FORCED VIBRATION MEASUREMENTS

In the previous section it was stated that the granular infills are able to absorb the vibrations generated in the floor (presumably by impacts). This can be shown experimentally from surface vibration measurements.

An electrodynamic shaker was used to provide a vertical force on the floor upper surface. The shaker was connected to the floor through a wire stinger and a reference force transducer. A scanning laser vibrometer (Polytec PSV 300) was used to measure the velocity of the floor and ceiling normal to the surface. A grid with a spatial resolution of 10-14cm was used to obtain a map of the surface velocity of the floor and ceiling relative to the input force; both amplitude and phase information was recorded at each frequency.

Figure 4 shows the results of the vibration measurements on the '85mm Sand/Sawdust Floor'. We can see how the vibration is quickly damped by the granular infill.

In comparison, Figure 5 shows the results of the vibration measurements on a floor with a floating gypsum concrete screed (Figure 15). We can how the vibration is not damped, and spreads over the whole floor. Careful edge detailing is therefore required to avoid severely reducing the floors sound insulation performance.

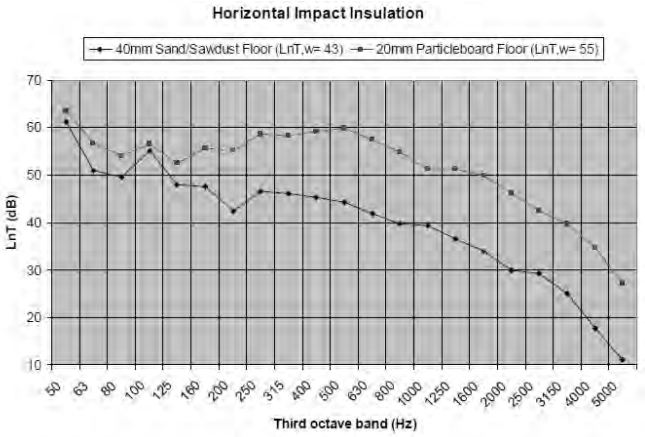

Figure 8. Horizontal impact sound insulation measurements.

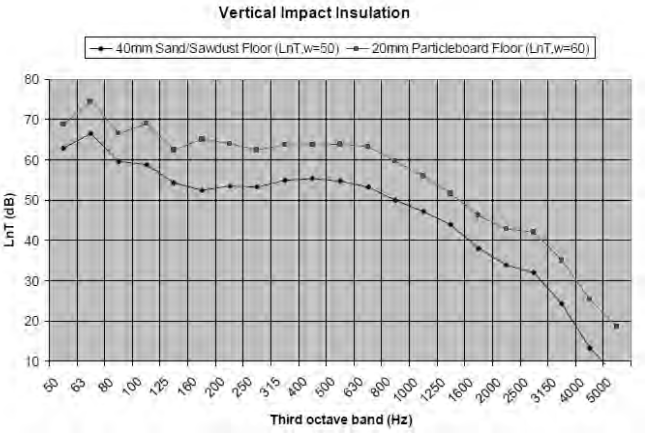

Figure 9. Vertical impact sound insulation measurements.

FLOOR/WALL SYSTEM MEASUREMENTS

The performance of a floor/wall system with a granular material-infilled floor topping was measured in the BRANZ four-room flanking test facility. The flanking facility was designed to test the sound insulation of a horizontal cruciform wall/floor system (Figure 6). All other sound paths were suppressed by the test facility (Emms & Walther, 2010). The measurements were done in accordance with standard ISO 140.

The system under test used the floor's 17mm plywood as a structural floor diaphragm. Hence, there was significant acoustic bridging for horizontal sound transmission . The wall consisted of a double-stud construction, with two layers of 13mm fire-rated plasterboard on each side (Figure 6). The subfloor construction is shown in Figure 7. On the subfloor a number of floor topping systems were trialled. The measurement results of two floor toppings are examined:

- 20mm particleboard screwed to the subfloor.
- 45mm deep battens screwed to subfloor, 40mm of sand/sawdust (80% / 20% by loose volume) infill between battens, and 20mm particleboard screwed to top of battens. Edges are constructed by butting battens against walls; no foam separation was used.

Measurement results

In the following figures we compare the sound insulation measurement results of the two floor toppings (i.e. 40mm sand/sawdust and 20mm particleboard).

We can see that the sand/sawdust mixture markedly improves the horizontal insulation performance (Figure 8 and Figure 10). Presumably this is due to a significant reduction in vibration energy being transmitted to the subfloor and across the continuous floor diaphragm. The horizontal airborne insulation performance of the system (Figure 10) with the 40mm sand/sawdust topping system is limited by the wall performance; whereas the sound transmitted via the floor flanking path limits performance in the 20mm particleboard system.

The sand/sawdust mixture also improves the vertical insulation performance (Figure 9 and Figure 11). This improvement is due to a combination of increased mass and damping in the floor topping reducing energy being transmitted to the ceiling and to the frame and wall.

CONCLUSION

In this paper the use of granular materials (specifically sand and sand/sawdust mixes) in floor topping systems have been considered. Recent measurement results were compiled and examined to show that these sorts of systems can significantly improve the sound insulation performance of the floor. The improved performance is due to increased vibration damping

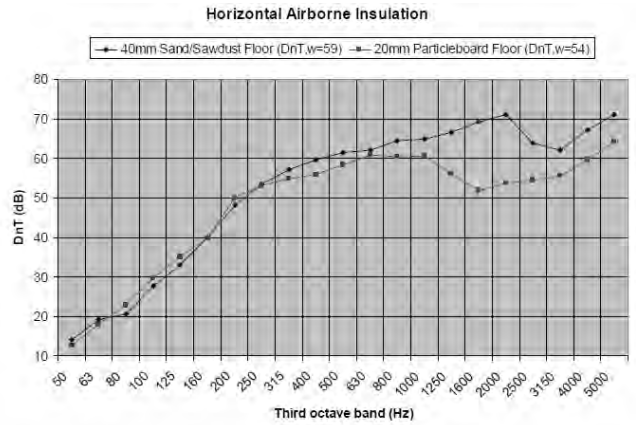

Figure 10. Horizontal airborne sound insulation measurements.

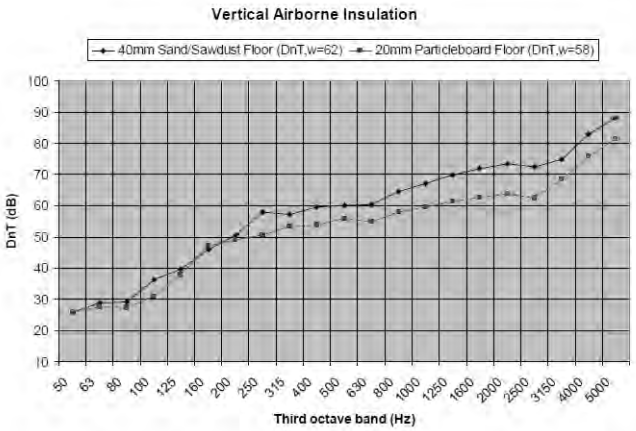

Figure 11. Vertical airborne sound insulation measurements.

and due to increased mass. As a result of these two factors, performance is improved across the whole frequency range.

It was also shown that the vibration damping effect localises impact vibrations, thereby reducing flanking transmission issues.

Another advantage such floor topping systems with granular infill is that they are not floating on the subfloor in any way. The topping is directly fixed to the subfloor, and there is no resilient isolation between layers. Edges are simply constructed by butting battens against walls – again no foam separation is used. All the isolation is achieved through vibration absorption in the granular material. It would appear, therefore, that it is an inherently robust system.

ACKNOWLEDGEMENTS

Thanks to George Dodd, Ken McGunnigle and Gian Schmid for helping to make the floor element measurements at the University of Auckland. Thanks to Tony Walther and Graeme Beattie for the opportunity to make the flanking transmission measurements at BRANZ, Judgeford, New Zealand.

REFERENCES

Emms, G., Chung, H., Dodd, G., McGunnigle, K., Schimd, G., (2006) Maximising impact sound resistance of timber framed floor/ceiling systems, Forest and Wood Products Research and Development Corporation (Australia), Project PN04.2005.

Emms, G. W.; Walther, T.; (2010). Flanking Transmission Measurements: Part 1- Measurement Techniques. Building Acoustics, Volume 17, Number 1, Pages 15–34

Kuhl, W., Kaiser, H. (1962). "Absorption of structureborne sound in building materials without and with sand-filled cavities", Acustica, 2, 179-188.

Lappert, A., Geinoz, D., (1998). "Experience in Multi-storey timber buildings consulting and field measurement", Proceedings of Acoustic Performance of Medium-rise Timber Buildings, Dublin, Ireland, Dec. 1998.

Richards, E. J., Lenzi, A. (1983). "On the prediction of impact noise, VII: The structural damping of machinery", Journal of Sound and Vibration, 97(4), 549-586.

Sun, J.C., Sun, H.B., Chow, L.C., Richards, E.J. (1986). "Predictions of total loss factors of structures, part II: Loss factors of sand-filled structure", Journal of Sound and Vibration, 104(2), 243-257.

Walk, M. & Keller, B. (2001). "Highly sound – insulating wooden floor system with granular filling", Proceedings of ICA 2001.

Xu, Z., Wang, M. Y., & Chen, T. (2005). Particle damping for passive vibration suppression: Numerical modelling and experimental investigation. Journal of Sound and Vibration, 279(3-5), 1097-1120. ¶

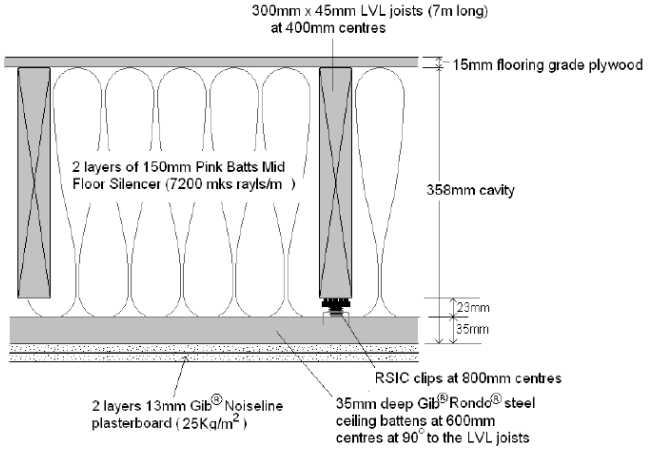

Figure 12. The 'Basic Floor' on which toppings were added.

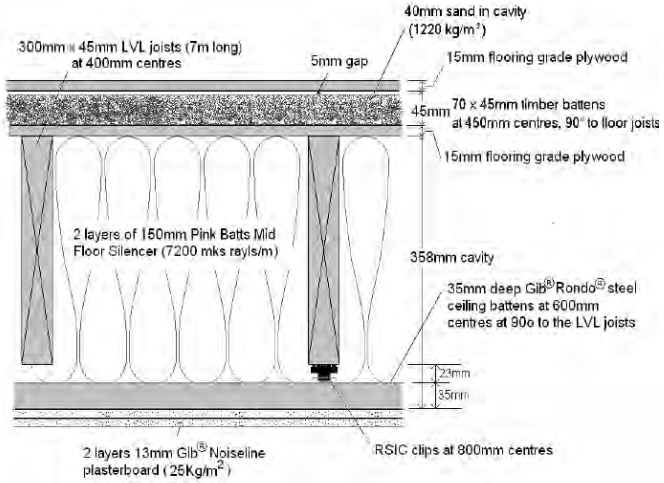

Figure 13. The '40mm Sand Floor'.

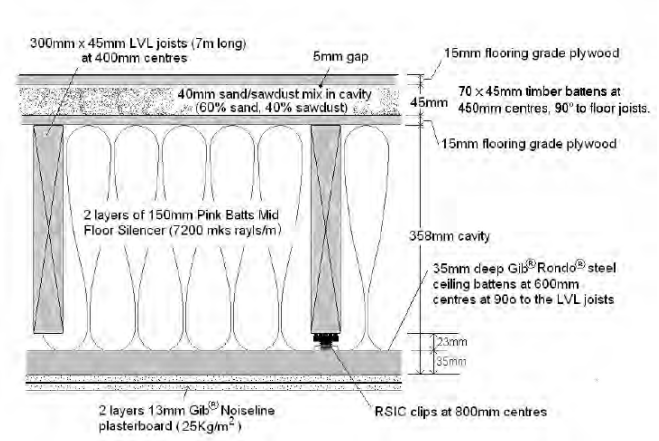

Figure 14. The '40mm Sand/Sawdust Floor'.

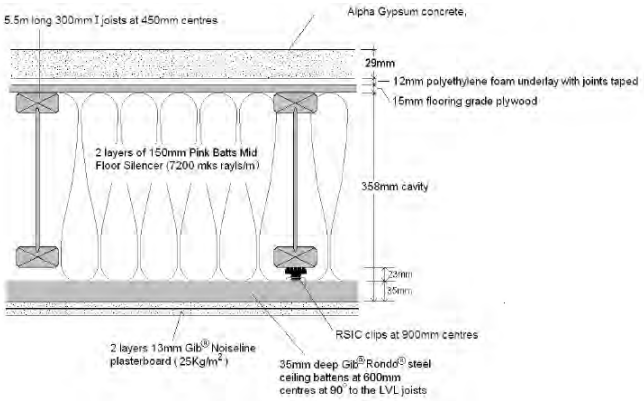

Figure 15. Floating Gypsum Concrete Floor.

VibraScout USB DC Triaxial Vibration Measurement System

Dytran Instruments, Inc. is an industry leader in the design and manufacture of piezoelectric and DC MEMS sensors to support a variety of vibration testing applications, including NVH, component durability, modal and structural analysis, flight vibration testing, seismic monitoring, road load data acquisition, transmission testing, ride quality and real time monitoring of plant & equipment, vehicles, sea going vessels and aircraft.

Included among the new Dytran DC MEMS sensors is the VibraScout Vibration Measurement System now available through Kingdom Pty Ltd, which includes a USB digital triaxial accelerometer combining a MEMS accelerometer with a microcontroller to create an intelligent sensor.

The VibraScout Vibration Measurement System consists of a USB triaxial DC response accelerometer, 15-foot 4-pin to USB cable assembly, VibraScout Data Acquisition Software, and VibraScout Windows compatible Post Processor software on CD (no license required). In addition to the vibration measurement system, the only required hardware is a personal computer with a USB port.

The accelerometer model features power from a PC bus, and as a result no additional external power supply is required. The software package supplied with each system allows for real time, three directional acceleration acquisition (including Static Inclination) along with real-time temperature monitoring. The standard USB protocol handles all the sensor communications with the PC and provides the following information: storage of acceleration and temperature data; real-time scrolling plots of acceleration data with display of min, max and mean; real-time logging of data to delimited file for importing into Excel; both auto & smart triggering modes; digital filters to improve signal/noise ratio; real-time compression to Fast Fourier Transform (FFT); and more.

The variable capacitance (VC) accelerometer combines an integrated VC chip in a hermetically sealed titanium housing weighing 17 grams which provides a 16g acceleration range and a low-end frequency response down to DC (0 Hz) with an upper frequency range of 1,100 Hz. Units are rugged to 10,000g shock and operate from +3.8 to +6.0 VDC power obtained from the computer through the USB connection.

The VibraScout Post Processor software is designed to provide a user with the tools to apply non-linear interpolation to resample raw data that is recorded with VibraScout software to higher frequencies, thus improving signal resolution. Data is valid only up to 1.1 kHz after applying the post processing.

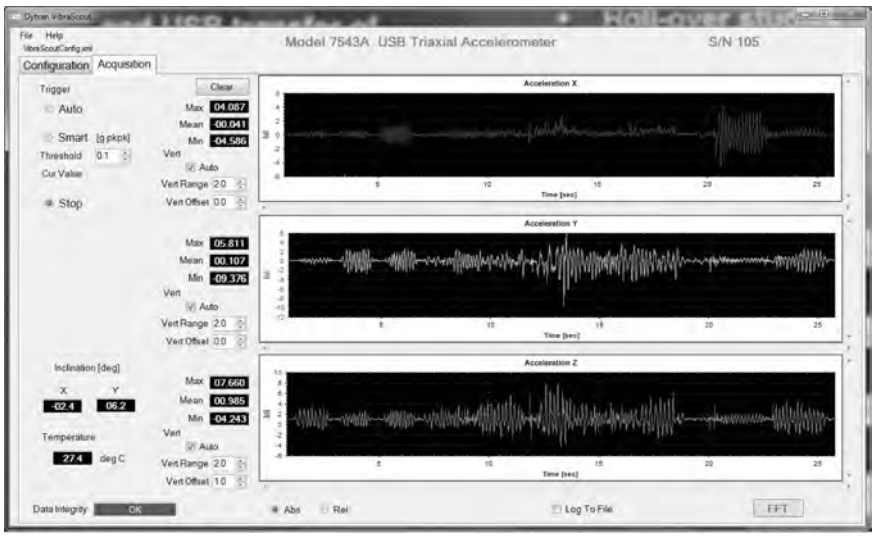

This mathematical interpolation is performed using the Whittaker-Shannon interpolation technique to reproduce the recorded real signals with proper amplitude.

Features of the VibraScout Post Processor software include: plot recorded data from the software; zoom and select a specific timeframe of recorded data for post processing; reproduce interpolated oversampled data to provide better resolution of vibration signals; multiple file types to export to including ASCII, time history .JPG files, TDMS binary files of time history data readable in Microsoft Excel, PSD and FFT plots in Joint Photographic file format; and display of recorded average temperature.

The VibraScout USB Vibration Measurement System was designed for a variety of low-to-medium frequency vibration applications where portability is critical including quick, easy in-field data collection; Noise, Vibration and Harshness (NVH); static angular measurements; ride quality; vibration measurement and diagnosis at rotating machinery; and simplified field data testing. The system is also ideal for calibration of sensors where qualification is required in the low range down to DC (0 Hz)

An Application Programming Interface (API) is available for customers who would like to build custom applications for the VibraScout. The API provides support for any .NET-compatible client applications. Custom application development is also available. Please contact Kingdom Pty Ltd directly for further information (kingdom9@kingdom.com.au). ¶

Acoustic Crossword #8

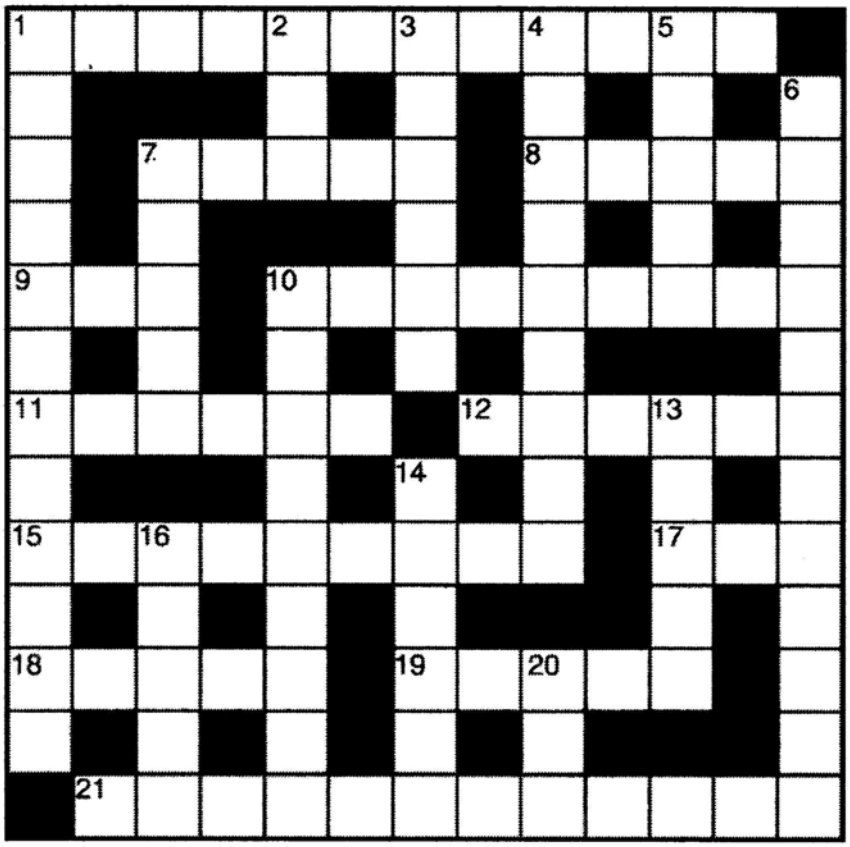

CLUES ACROSS

1. Party poopers lose love but softly gain some celebratory noise makers (5,7)
7. George Bernard Shaw regarded it as the brandy of the damned when taken aurally rather than orally (5)
8. Where we find the claim of a virgin birth in scattered décor (5)
9. Add on six balls and it is frequently what we do at Christmas dinner (3)
10. And 19 across Are these where Dec 25th grows? (9,5)
11. A tuner possibly finds many sounds in here (6)
12. One who mitigates their nuisance using a mixture of bat and oar (6)
15. Because she didn't hear it Nora gets involved in crash (1,4,4)
17. It's got both 8 dB and 32 dB rules and could be a manufacturer of early English microphones (3)
18. The divisor for converting angular frequency to frequency in Hz (3,2)
19. See 10 across
20. An unmarried female with undesirable fat has charge for making a passage of sound through a wall (12)

CLUES DOWN

1. The angelic Christmas message which gladdens the hearts of members of the Noise Abatement Society (5,2,5)
2. The affirmative is given in a noisy escapade (3)
3. Romeo's car sound features in the Academy awards (6)
4. 10-12 m^2 of total absorption (9)
5. Sounds of crying or sneezing can accompany of this when he gets into rum (5)
6. The noise from this is the subject of NZS 6803 (12)
7.She might be sung at Christmas in this polyphonic unaccompanied form (5)
10. Jesus was not one but people who honour him at Christmas often are (9)
13. Cricket or acoustics verifications? (5)
14. The sound of an explosion envelopes an abstainer for a weaver in a Mid-Summer Nights Dream (6)
16. How a romantic acoustician might fancifully imagine 20 micropascals in a game of French tennis? (5)
20. Where to send your Sound Level Meter for calibration (3)

Solutions to Crossword #7

Across:

1. Hard of
4. Herald
9. Moved
10. Eardrum
12. Echo
14. Bels
17. Data
22. Manage
23. Nodes

Down:

1. Hammer
2. Reverberation
3. Order
5. Enhance
13. Hearing
16. Alarms
19. Raven

Crossword submitted by:

Dogged Doer

Crying & Autism

The acoustics of a baby's cry may serve as one indicator of whether an infant will develop autism, according to a recent study conducted at Brown University, USA.

"A major challenge in research in autism is how we can identify autism in early infancy," said Stephen Sheinkopf, assistant professor of psychiatry and human behavior and lead author of the study, published in the October issue of the journal of Autism Research.

Sheinkopf and his fellow researchers examined the naturally occurring cries of about 40 six-month-old infants, representing two subject groups. One group was identified as high-risk for Autism Spectrum Disorder because the subjects had an older sibling with the disease. The second group was identified as low-risk for autism because the subjects had no siblings who had the disorder.

Recordings of the cries were made using a camcorder and microphone embedded in a vest worn by each infant at home, according to the study. Once recorded, the cries were categorized into pain-related and non-pain-related cries. The pitch of the cries was identified using a program specifically designed for the study.

When the researchers compared the pitches of the pain-related cries from both groups they found that the cries of the high-risk infants on average had a statistically significant higher pitch than the cries of low-risk infants. In fact, the three infants in the high-risk group who did develop autism were the subjects with the three highest-pitched cries, he said. No statistically significant difference in acoustic features was found for the non-pain-related cries, according to the study.

"Atypical cry acoustics ... may serve as a positive symptom that, when combined with other indices of risk, may have additional value as a means to increase the accuracy of early identification efforts," the study states.

One of the study's major strengths was its approach while using naturalistic observation. Most cry acoustic studies evoke cries systematically to gather data. The experimental design of this study, in which cries were observed "naturalistically," was a new approach to collecting cry acoustic data.

The authors noted that the study's small sample size was a weakness. The biggest challenge was identifying prospective high-risk infants – a difficult task given that autism is not diagnosed until age two, Sheinkopf said.

A reviewer recommended that the researchers reevaluate the infants when they are 36 months old to see if the infants with Autism Spectrum Disorder still have a higher-pitched cry.

© Adapted from an article by Phoebe Draper

The Brown Daily Herald

Sound Snippets: Speaking with Your Hands

Gestures and Speech

People of all ages and cultures gesture while speaking, some much more noticeably than others. But is gesturing uniquely tied to speech, or is it, rather, processed by the brain like any other manual action?

A U.S.-Netherlands research collaboration delving into this tie discovered that actual actions on objects, such as physically stirring a spoon in a cup, have less of an impact on the brain's understanding of speech than simply gesturing as if stirring a spoon in a cup. This is surprising because there is less visual information contained in gestures than in actual actions on objects. In short: Less may actually be more when it comes to gestures and actions in terms of understanding language.

Spencer Kelly, associate professor of Psychology, director of the Neuroscience program, and co-director of the Center for Language and Brain at Colgate University, and colleagues from the National Institutes of Health and Max Planck Institute for Psycholinguistics presented their research at the Acoustics 2012 meeting in Hong Kong, May 13-18, a joint meeting of the Acoustical Society of America (ASA), Acoustical Society of China, Western Pacific Acoustics Conference, and the Hong Kong Institute of Acoustics.

Continued on Page 34...

...Continued from Page 32

Among their key findings is that gestures – more than actions – appear to make people pay attention to the acoustics of speech. When we see a gesture, our auditory system expects to also hear speech. But this is not what the researchers found in the case of manual actions on objects.

Just think of all the actions you've seen today that occurred in the absence of speech. "This special relationship is interesting because many scientists have argued that spoken language evolved from a gestural communication system – using the entire body – in our evolutionary past," points out Kelly.

"Our results provide a glimpse into this past relationship by showing that gestures still have a tight and perhaps special coupling with speech in present-day communication. In this way, gestures are not merely add-ons to language – they may actually be a fundamental part of it."

A better understanding of the role hand gestures play in how people understand language could lead to new audio and visual instruction techniques to help people overcome major challenges with language delays and disorders or learning a second language.

What's next for the researchers? "We're interested in how other types of visual inputs, such as eye gaze, mouth movements, and facial expressions, combine with hand gestures to impact speech processing. This will allow us to develop even more natural and effective ways to help people understand and learn language," says Kelly.

ASA's World Wide Press Room

(www.acoustics.org/press)

ACOUSTIC CEILING TILES

AMF THERMATEX ACOUSTIC RANGE

The new AMF Acoustic Range offers ceiling tiles with a choice of high and low sound absorption with a uniform face pattern.

- One face pattern for a spectrum of sound absorption values
- Tile options from low to high absorption
- Attenuation figures from 26 dB to 44 dB
- A combination of acoustic properties in one suspended ceiling
- Building material class A2-s1, d0 as per EN 13501-1

THERMATEX ACOUSTIC RANGE

Thermatex	NRC	dB
Alpha One	1.00	29
Silence	0.90	44
Alpha	0.90	26
Thermofon	0.85	28
Alpha HD	0.85	30
Acoustic	0.70	38
dB Acoustic 24mm	0.70	41
Acoustic RL	0.15	38

as per EN ISO 11654 / EN 20140-9 / ASTM C 423

For more information, contact Potter Interior Systems today!
0800 POTTERS
www.potters.co.nz
info@potters.co.nz

Upcoming Events

2013

26 - 31 March, Vancouver, Canada. 2013 IEEE International Conference on Acoustics, Speech, and Signal Processing (ICASSP)
http://www.icassp2013.com

1 - 4 May, Singapore 3rd International Congress on Ultrasonics (ICU 2013) concurrently organized with the 32nd International Symposium on Acoustical Imaging (AI 2013)
http://www.epc.com.sg/PDF%20Folder/ICU%202010%20Phamplet%20v1%20(12%20Jul%202010).pdf

2 - 7 June, Montreal, Canada 21st International Congress on Acoustics(ICA 2013)
http://www.ica2013montreal.org

1-3 July 2013, International Conference on Recent Advances in Structural Dynamics, RASD 2013

Colleagues,
RASD will be held at the University of Pisa, Pisa, Italy, 1-3 July 2013. The eleventh in the RASD series, the conference will bring together researchers working in all areas of structural dynamics. The ten previous conferences have been held every three years or so since 1980.

As on prevision occasions, this conference is devoted to theoretical, numerical and experimental developments in structural dynamics and their application to all types of structures and dynamical systems. It will be an opportunity to exchange scientific, technical and experimental ideas.

The Call for Papers will be made in June 2012 with the deadline for the submission of abstracts being 28th September 2012. Submission and Registration to the conference will be done through the University of Southampton Open Conference System (www.ocs.soton.ac.uk/index.php/rasdconference/RASD2013).

Dr Emiliano Rustighi (on behalf of the RASD2013 Organising Committee)

Further information is available at https://www.soton.ac.uk/rasd2013

7-11 July 2013, 20th International Congress on Sound and Vibration (ICSV20), Bangkok, Thailand

The 20th International Congress on Sound and Vibration (ICSV20) will be held 7-11 July 2013 in Bangkok, Thailand. The ICSV20 is sponsored by the International Institute of Acoustics and Vibration (IIAV) and the Faculty of Science; Chulalongkorn University, the Acoustical Society of Thailand and the Science Society of Thailand; the ICSV20 is organized in cooperation with: the International Union of Theoretical and Applied Mechanics; the American Society of Mechanical Engineers International and the Institution of Mechanical Engineers. The ICSV20 Congress will be held at Imperial Queens Park Hotel, Bangkok, Thailand.

Theoretical and experimental papers in the fields of acoustics, noise, and vibration are invited for presentation. Participants are welcome to submit abstracts to www.icsv20.org and companies are invited to take part in the ICSV20 exhibition and sponsorship. For more information, please visit: http://www.icsv20.org

11-12 July 2013, The ISVR at 50

2013 will mark the 50th anniversary of the foundation of the Institute of Sound and Vibration Research, at the University of Southampton, UK.

To celebrate the achievements of its people, past and present, we will be hosting a two-day symposium on the 11th and 12th July 2013.

The symposium will feature talks from key speakers having an association with the ISVR, and will also include our annual E J Richards lecture. The celebrations will culminate in a social function with a buffet supper and entertainment. The tickets for the event are £50 for full attendance, with a reduced cost for partial attendance.

Details of the event are available online at http://www.isvr.co.uk/ISVR-50th-anniversary

26 - 28 August, Denver, USA NOISE-CON 13, 27 - 30 August, Denver, USAWind Turbine Noise 2013
http://www.inceusa.org

15 - 18 September, Innsbruck, Austria Internoise 2013
http://www.internoise2013.com

9-11 October, Hangzhou, China 4th Pacific Rim Underwater Acoustics Conference (PURAC 2013)
http://pruac.zju.edu.cn/index.htm

2 - 6 December, San Francisco, USA 166th Meeting of the Acoustical Society of America
http://www.acousticalsociety.org

2014

5 - 9 May, Providence, USA 167th Meeting of the Acoustical Society of America
http://www.acousticalsociety.org

6 - 10 July, Beijing, China 21th International Congress on Sound and Vibration (ICSV21)

27 - 31 October, Indianapolis, USA 168th Meeting of the Acoustical Society of America
http://www.acousticalsociety.org

16 - 19 November, Melbourne, Australia Internoise 2014
http://www.internoise2014.org

CRAI Ratings

Auckland

215, Dominion Rd	(1)	★★★★½
Andrea (form. Positano), Mission Bay	(1)	★★★
Aubergine's, Albany	(1)	★★★★½
Backyard, Northcote	(1)	★★
Bask, Browns Bay	(1)	★★★
Bay (The), Waiake, North Shore	(1)	★★★★★
Bolero, Albany	(1)	★★★★
Bosco Verde, Epsom	(1)	★★★★½
Bouchon, Kingsland	(1)	★★
Bowman, Mt Eden	(2)	★★★★½
Bracs, Albany	(1)	★★★★
Brazil, Karangahape Rd	(1)	★★★
Buoy, Mission Bay	(2)	★★★★½
Byzantium, Ponsonby	(1)	★★★
Café Jazz, Remuera	(1)	★★★★½
Carriages Café, Kumeu	(1)	★★★★
Charlees, Howick	(1)	★★★★★
Cibo	(1)	★★★★★
Circus Circus, Mt Eden	(2)	★★
Cube, Devenport	(1)	★★
Del Fontaine, Mission Bay	(1)	★★★★★
Deli (The), Remuera	(1)	★★★★
Delicious, Grey Lynn	(1)	★★★★★
De Post, Mt Eden	(1)	★★
Dizengoff, Ponsonby Rd	(1)	★★
Drake, Freemans Bay (Function Room)	(1)	★★
Eiffel on Eden, Mt Eden	(1)	★★
Eve's Cafe, Westfield Albany	(1)	★★★½
Formosa Country Club Restaurant	(1)	★★★★★
Garrison Public House, Sylvia Park	(1)	★★★★½
Gee Gee's	(1)	★★★
Gero's, Mt Eden	(9)	★★★
Gina's Pizza & Pasta Bar	(1)	★★★½
Gouemon, Half Moon Bay	(1)	★★
Hardware Café, Titirangi	(1)	★★★★★
Hollywood Café, Westfield St Lukes	(1)	★★½
IL Piccolo	(1)	★★★★
Ima, Fort Street	(1)	★★★★
Jervois Steak House	(1)	★★★
Kashmir	(1)	★★★★
Katsura	(1)	★★★½
Khun Pun, Albany	(2)	★★★★★
Kings Garden Ctre Café, Western Springs	(1)	★★
La Tropezienne, Browns Bay	(1)	★★
Malaysia Satay Restaurant, Nth Shore	(1)	★★★★★
Mecca, Newmarket	(1)	★★★★★
Mexicali Fresh, Quay St	(1)	★★
Mezze Bar, Little High Street	(16)	★★★★
Monsoon Poon	(1)	★★★★★
Mozaike Café, Albany	(1)	★★
Nana Thai, Botany South	(1)	★★★★½
Narrow Table (The), Mairangi Bay	(1)	★★★★½
One Red Dog, Ponsonby	(1)	★★★
One Tree Grill	(2)	★★★★
Orbit, Skytower	(2)	★★★★
Pakuranga Thai	(1)	★★★★★
Patriot, Devonport	(1)	★★★½
Pavia, Pakuranga	(1)	★★★★★
Prego, Ponsonby Rd	(2)	★★
Remuera Rm, Ellerslie Racecourse	(1)	★★★★★
Rhythm, Mairangi Bay	(1)	★★
Rice Queen, Newmarket	(12)	★★★★
Sails, Westhaven Marina	(2)	★★★★★
Scirocco, Browns Bay	(1)	★★★
Seagers, Oxford	(1)	★★★★
Shahi, Remuera	(1)	★★★½
Shamrock Cottage, Howick	(1)	★★
Sidart, Ponsonby	(1)	★★★★½
Sitting Duck, Westhaven	(1)	★★★½
Sorrento	(1)	★★½
Spices Thai, Botany South	(1)	★★★★
Stephan's, Manukau	(1)	★★★★★
Tempters Café, Papakura	(1)	★★★★★
Thai Chef, Albany	(1)	★★★★★
Thai Chilli	(1)	★★★★★
Thai Corner, Rothesay Bay	(1)	★★★★★
Tony's, High St	(1)	★★★
Traffic Bar & Kitchen	(1)	★★
Umbria Café, Newmarket	(1)	★★★★½
Valentines, Wairau Rd	(1)	★★★★★
Vivace, High Street	(2)	★★½
Wagamama, Newmarket	(1)	★★★★½
Watermark, Devonport	(1)	★★
Woolshed, Clevedon	(1)	★★½
Zarbos, Newmarket	(1)	★★
Zavito, Mairangi Bay	(1)	★★ ★

Arthur's Pass

Arthur's Pass Cafe & Store	(1)	★★★½
Ned's Cafe, Springfield	(1)	★★★★

Ashburton

Ashburton Club & MSA	(1)	★★★★½

Readers are encouraged to rate eating establishments which they visit by completing a simple form available on-line from www.acoustics.ac.nz, or contact the Editor.
Repeat ratings on listed venues are encouraged.

★ Lip-reading would be an advantage. ★★ Take earplugs at the very least. ★★★ Not too bad, particularly mid-week. ★★★★A nice quiet evening. ★★★★★The place to be and be heard. (n) indicates the number of ratings.

CRAI Ratings (cont.)

Robbies	(1)	★★★
RSA	(1)	★★★★
Tuscany Café & Bar	(1)	★★★

Bay of Plenty

Alimento, Tauranga	(1)	★½
Imbibe, Mt Maunganui	(1)	★½
Versailles Café, Tauranga	(2)	★★

Blenheim

Raupo Cafe	(1)	★★

Bulls

Mothered Goose Cafe, Deli, Vino	(1)	★★

Cambridge

GPO	(1)	★★★★★

Christchurch

@Tonys, Ferrymead	(6)	★★½
3 Cows, Kaiapoi	(1)	★★★★
Abes Bagel Shop, Mandeville St	(1)	★★★★
Addington Coffee Co-op	(4)	★★★★
Alchemy Café, Art Gallery	(1)	★★★★★
Anna's Café, Tower Junction	(1)	★★★★
Arashi	(1)	★★
Azure	(2)	★★★
Bamboozle, Sumner	(5)	★★½
Becks Southern Ale House	(11)	★★★★½
Buddha Stix, Riccarton	(1)	★★★★
Bully Haye's, Akaroa	(1)	★★
Cashmere Club	(1)	★★★★★
Cassels & Sons, The Brewery	(5)	★★★★
Christchurch Casino	(1)	★★
Christchurch Museum Café	(1)	★★★★
Cobb & Co, Bush Inn	(1)	★★★
Coffee House, Montreal Street	(1)	★★
Cookai	(3)	★★½
Corianders, Edgeware Road	(11)	★★★
Decadence Café, Victoria St	(1)	★★★★★
Drexels Breakfast Restaurant, Riccarton	(1)	★★★★
Edisia, Addington	(1)	★★★
Elevate, Cashmere	(1)	★★★
Fava, St Martins	(1)	★★
Flying Burrito Brothers, Northlands	(12)	★★½
Foo San, Upper Riccarton	(1)	★★★½
Fox & Ferrett, Riccarton	(1)	★★★★★
Gloria Jean's, Rotheram St	(1)	★★★★
Golden Chimes	(1)	★★★★★
Governors Bay Hotel	(1)	★★★★
Green Turtle	(1)	★★★★
Harpers Café, Bealey Ave	(1)	★★★★★
Holy Smoke, Ferry Rd	(1)	★★
Indian Fendalton	(2)	★★
JDV, Merivale	(2)	★★★★
Kanniga's Thai	(1)	★★★
La Porchetta, Riccarton	(4)	★★½
Lone Star, Northlands	(1)	★★★
Lone Star, Riccarton Road	(6)	★★★
Lyttleton Coffee Co, Lyttleton	(1)	★★★★
Manee Thai	(6)	★★½
Mexican Café	(6)	★★★
Myhanh, Church Corner	(4)	★★★½
Number 4, Merivale	(2)	★★★★
Oasis	(1)	★★★★½
Old Vicarage	(2)	★★★½
One Good Horse, Parklands	(4)	★★★★
Phu Thai, Manchester Street	(1)	★★★
Pukeko Junction, Leithfield	(1)	★★★★
Red, Beckenham Service Centre	(1)	★★★★
Red Elephant	(1)	★★★★
Retour	(1)	★★★
Riccarton Buffet	(2)	★★★★½
Robbies, Church Corner	(2)	★★★★½
Route 32, Cust	(1)	★★★★
Saggio di Vino (2012)	(1)	★★★★½
Salt on the Pier, New Brighton	(6)	★★★½
Speights Ale House, Tower Junction	(1)	★★★★
Spice 'n' Life, Church Corner	(4)	★★★★½
The Bridge, Prebbleton	(1)	★★★★★

The Sand Bar, Ferrymead	(2)	★★★½
Tokyo Samurai	(1)	★★★★★
Tutto Bene, Merivale	(2)	★★
Untouched World Cafe	(1)	★★★★★
Waitikiri Golf Club	(1)	★★
Waratah Café, Tai Tapu	(1)	★★★

Clyde

Old Post Office Cafe	(1)	★★★★★

Dunedin

A Cow Called Berta	(1)	★★★½
Albatross Centre Cafe	(1)	★★★★★
Bennu	(1)	★★★★
Bx Bistro	(1)	★★★★
Chrome	(1)	★★★★½
Conservatory, Corstophine House	(1)	★★★★★
Fitzroy Pub on the Park	(1)	★★★★★

CRAI Ratings (cont.)

High Tide	(2)	★★
Nova	(1)	★★★★★
St Clair Saltwater Pool Cafe	(1)	★★★★½
Swell	(1)	★★
University of Otago Staff Club	(1)	★★

Feilding

Essence Cafe & Bar	(1)	★★★★

Gore

Old Post	(1)	★★★
The Moth, Mandeville	(1)	★★★★★

Greymouth

Cafe 124	(1)	★★★

Hamilton

Embargo	(1)	★★★★★
Gengys	(1)	★★
Victoria Chinese Restaurant	(1)	★★★★★

Hanmer Springs

Laurels (The)	(2)	★★★★★
Saints	(1)	★★★★½

Hastings

Café Zigliotto	(1)	★★★

Havelock North

Rose & Shamrock	(1)	★★★½

Levin

Traffic Bar & Bistro	(1)	★★

Masterton

Java	(1)	★★

Matamata

Horse & Jockey	(1)	★★★★★

Methven

Ski Time	(2)	★★★

Napier

Boardwalk Beach Bar	(2)	★★★★★
Brecker's	(1)	★★★★★
Café Affair	(1)	★★
Cobb & Co	(1)	★½
Duke of Gloucester	(1)	★★★★½
East Pier	(1)	★★
Estuary Restaurant	(1)	★★★★★
Founder's Cafe	(1)	★★★★★
Napier RSA	(1)	★★★★★
Sappho & Heath	(1)	★★

Nelson/Marlborough

Allan Scott Winery	(1)	★★★★★
Amansi @ Le Brun	(1)	★★★★★
Baby G's, Nelson	(1)	★★★★★
Boutereys, Richmond	(1)	★★★★
Café Affair, Nelson	(1)	★★
Café on Oxford, Richmond	(1)	★★★
Café Le Cup, Blenheim	(1)	★★★
Crusoe's, Stoke	(1)	★★★
Cruizies, Blenheim	(2)	★★★★½
Grape Escape, Richmond	(1)	★★★★★
Jester House, Tasman	(1)	★★★★★
L'Affaire Cafe, Nelson	(1)	★★
Liquid NZ, Nelson	(1)	★½
Lonestar, Nelson	(1)	★★★★
Marlborough Club, Blenheim	(1)	★★
Morrison St Café, Nelson	(1)	★★½
Oasis, Nelson	(1)	★★★★★
Rutherford Café & Bar, Nelson	(1)	★★★★★
Suter Cafe, Nelson	(1)	★★
Verdict, Nelson	(1)	★★
Waterfront Cafe & Bar, Nelson	(1)	★★★
Wholemeal Trading Co, Takaka	(1)	★★★★★

New Plymouth

Breakers Café & Bar	(1)	★★★
Centre City Food Court	(1)	★★★★
Elixer	(1)	★★★★
Empire Tea Rooms	(1)	★★★★½
Govett Brewster Cafe	(1)	★★
Marbles, Devon Hotel	(1)	★★★
Pankawalla	(1)	★★★★★
Simplicity	(1)	★★★
Stumble Inn, Merrilands	(1)	★★★
Yellow Café, Centre City	(1)	★★★
Zanziba Café & Bar	(1)	★★★

Oamaru

Riverstone Kitchen	(1)	★★★★★
Star & Garter	(1)	★★★
Woolstore Café	(1)	★★★★

Palmerston North

Café Brie	(1)	★★★
Café Esplanade	(2)	★★★★
Chinatown	(1)	★★★★
Coffee on the Terrace	(2)	★★★
Elm	(1)	★★★★½
Fishermans Table	(1)	★★★★★
Gallery	(3)	★★★★

CRAI Ratings (cont.)

Rendezvous	(1)	★★½
Roma Italian Restaurant	(1)	★★★
Rose & Crown	(1)	★★
Tastee	(1)	★★★
Thai House Express	(1)	★★★★★
Victoria Café	(1)	★★★★

Queenstown

Bunker	(1)	★★★★
The Cow	(1)	★★★
Sombreros	(1)	★
Tatler	(1)	★★★★
Winnies	(1)	★★★★★

Rotorua

Cableway Rest. at Skyline Skyrides	(1)	★★★★★
Lewishams	(1)	★★★
Woolly Bugger, Ngongotaha	(1)	★★★
Valentines	(1)	★★★★★
You and Me	(1)	★★★★★
Zanelli's	(1)	★★

Southland

Lumberjack Café, Owaka	(1)	★★★★★
Pavilion, Colac Bay	(1)	★★
Village Green, Invercargill	(1)	★★★★★

Taihape

Brown Sugar Café	(1)	★★★★½

Taupo

Burbury's Café	(1)	★★★
Thames		
Thames Bakery	(1)	★★★
Waiheke Island		
Cortado Espresso Bar	(1)	★★★★
Cats Tango, Onetangi Beach	(1)	★★★★

Timaru

Fusion	(1)	★★★★★

Wanganui

3 Amigos	(1)	★★★½
Bollywood Star	(1)	★★★½
Cosmopolitan Club	(1)	★★★★
Liffiton Castle	(1)	★★½
RSA	(1)	★★★½
Stellar	(1)	★★★★½
Wanganui East Club	(1)	★★★★

Wellington

162 Café, Karori	(1)	★★★★★
180°, Paraparaumu Beach	(1)	★★
88, Tory Street	(35)	★★
Anise, Cuba Street	(1)	★★
Aranya's House	(1)	★★★★★
Arbitrageur	(2)	★★★
Arizona	(1)	★★
Astoria	(2)	★★★
Backbencher, Molesworth Street	(1)	★★★
Bordeaux Bakery, Thorndon Quay	(1)	★★
Brown Sugar, Otaki Railway Station	(1)	★★★
Buzz, Lower Hutt	(1)	★★½
Brewery Bar & Restaurant	(5)	★★★★
Carvery, Upper Hutt	(1)	★★★★★
Chow	(1)	★½
Cookies, Paraparumu Beach	(1)	★★★½
Cosa Nostra Italian Trattoria, Thorndon	(1)	★★★★
Dockside	(1)	★★★★
Gotham	(6)	★★★½
Great India, Manners Street	(2)	★★★★★
Habebie	(1)	★★
Harrisons Garden Centre, Peka Peka	(1)	★★★★
Hazel	(1)	★★
Katipo	(1)	★★★★★
Kilim, Petone	(4)	★★★★½
Kiss & Bake Up, Waikanae	(1)	★★★
La Casa Pasta	(1)	★★★★½
Lattitude 41	(3)	★★★★
Legato	(1)	★★
Le Metropolitain	(1)	★★★★★
Loaded Hog	(5)	★★★★½
Manhatten, Oriental Bay	(1)	★★★★
Maria Pia's	(1)	★★★
Matterhorn	(1)	★★★
Meow Café	(1)	★★
Mungavin Blues, Porirua	(1)	★★★★★
Olive Café	(1)	★★★★★
Olive Grove, Waikanae	(1)	★★★½
Original Thai, Island Bay	(1)	★★★★
Palace Café, Petone	(1)	★★½
Parade Café	(1)	★★
Pasha Café	(1)	★★★★
Penthouse Cinema Café	(2)	★★★½
Pod	(1)	★★½
Rose & Crown	(1)	★★★★★
Shed 5	(1)	★★
Siem Reap	(1)	★★
Speak Easy, Petone	(1)	★★
Speights Ale House	(1)	★★
Sports Bar Café	(1)	★★★★
Stanley Road	(1)	★★★
Stephan's Country Rest., Te Horo	(1)	★★★★★
Wakefields (West Plaza Hotel)	(1)	★★★
Windmill Café & Bar, Brooklyn	(1)	★★
Yangtze Chinese	(1)	★★★★½
Zealandia Café, Karori Sanctuary	(1)	★★★½

In a Class *of its Own*

The unmistakable look of Hand-held Analyzer Type 2270 can overshadow a number of discrete yet significant distinctions which make this powerful instrument the complete toolbox for sound and vibration professionals. These include:

- Integrated digital camera
- Two-channel measurement capability
- Integrated LAN and USB interfaces for fast data transfer to PC and remote control and monitoring of Type 2270
- Environmental protection IP44

Versatile in the Extreme

Type 2270 also boasts a wide range of application software modules that can be licensed separately so you get what you need when you need it.

Currently available measurement software includes:

- Sound Level Meter application
- Real-time frequency analysis
- Logging (noise level profiling)
- Sound and vibration recording
- Building acoustics
- Tonal assessment

Type 2270 meets the demands of today's wide-ranging sound and vibration measurement tasks with the accuracy and reliability associated with Brüel & Kjær instrumentation.

To experience the ease-of-use of Type 2270, just go to www.bksv.com and view the on-line video demonstrations.

For more information please contact your local Brüel & Kjær representative

Hand-held Analyzer *Type 2270*

Brüel & Kjær

New Zealand Agent:
Ross McBeath, Avia Ltd, PO Box 76 068, Manukau City, Auckland
Tel: +64 9 279 8802 Fax: +64 0 279 8883 E-mail: ross.mcbeath@avia.net.nz

NCS Acoustics

DESIGN • MANUFACTURE • INSTALL

PERFORMANCE GUARANTEED — Designed, manufactured and tested in New Zealand

ESTABLISHED — Formerly NOISE CONTROL SERVICES LTD — SINCE 1981

DESIGN

Got a commercial or industrial noise problem? Our acoustic engineers will design an economical, innovative solution to your exact requirements.

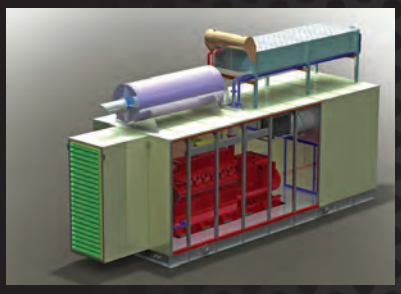

MANUFACTURE

Operating from a 2000m^2 purpose built factory in Auckland, we are able to meet the production requirements, large or small, of clients throughout New Zealand and internationally.

INSTALL

We offer installation, testing, monitoring and maintenance services, to ensure you receive optimum performance from our products.

We provide custom made acoustic solutions

- Attenuators: Rectangular, Cylindrical, Compact Cylindrical, Crosstalk, Curb
- Silent Supply/Extract Systems
- Acoustic Louvres
- Sound Enclosures, Canopies and Acoustic Containers
- Absorptive and Reactive Mufflers
- Blower, Vent and Specialist Diary Industry Silencers
- Acoustic Doors and Plugs
- Acoustic Barriers and Screens
- Absorption Panels
- Audiometric Booths

"If it's noisy we can fix it!"

P +64 9 269 0001
info@ncsacoustics.co.nz
www.ncsacoustics.co.nz

FORMERLY... NOISE CONTROL SERVICES — ACOUSTIC PRODUCTS AND DESIGN

Leaders in design, manufacture and installation of acoustic solutions.